



## Lateglacial and early Holocene evolution of the Tyne Valley in response to climatic shifts and possible paraglacial landscape legacies

Yorke, Lynda; Chiverrell, Richard; Schwenninger, Jean-Luc

### Geomorphology

DOI:

[10.1016/j.geomorph.2023.109007](https://doi.org/10.1016/j.geomorph.2023.109007)

Published: 01/02/2024

Peer reviewed version

[Cyswllt i'r cyhoeddiad / Link to publication](#)

*Dyfyniad o'r fersiwn a gyhoeddwyd / Citation for published version (APA):*

Yorke, L., Chiverrell, R., & Schwenninger, J.-L. (2024). Lateglacial and early Holocene evolution of the Tyne Valley in response to climatic shifts and possible paraglacial landscape legacies. *Geomorphology*, 446, Article 109007. <https://doi.org/10.1016/j.geomorph.2023.109007>

#### Hawliau Cyffredinol / General rights

Copyright and moral rights for the publications made accessible in the public portal are retained by the authors and/or other copyright owners and it is a condition of accessing publications that users recognise and abide by the legal requirements associated with these rights.

- Users may download and print one copy of any publication from the public portal for the purpose of private study or research.
- You may not further distribute the material or use it for any profit-making activity or commercial gain
- You may freely distribute the URL identifying the publication in the public portal ?

#### Take down policy

If you believe that this document breaches copyright please contact us providing details, and we will remove access to the work immediately and investigate your claim.

1 Lateglacial and early Holocene evolution of the Tyne Valley in response to climatic  
2 shifts and possible paraglacial landscape legacies.

3

4 Yorke, L.<sup>1</sup>, Chiverrell, R.C.<sup>2</sup> and Schwenninger, J-L.<sup>3</sup>

5 <sup>1</sup>School of Environmental & Natural Sciences, Bangor University, Thoday Building, Bangor, LL57  
6 2UW.

7 <sup>2</sup>Department of Geography and Planning, School of Environmental Sciences, University of  
8 Liverpool, Roxby Building, Liverpool, L69 7ZT.

9 <sup>3</sup>Research Laboratory for Archaeology and the History of Art, School of Archaeology, University of  
10 Oxford, Dyson Perrins Building, Oxford, OX1 3QY.

11

## 12 **Abstract**

13 This paper presents new sedimentological, geomorphological, and optically stimulated  
14 luminescence (OSL) geochronological evidence for fluvial evolution of the mid- to lower River  
15 Tyne through the Lateglacial to late Holocene. These data reveal a series of fluvial terraces  
16 produced by cycles of aggradation and incision, conditioned by glacial inheritance and driven by  
17 changing sediment availability and hydrological regime. The distribution and stratigraphy (where  
18 available) of nine river terrace and their associated sediments have been recorded. At two key  
19 sites the sediments have been dated using OSL measurements to constrain the fluvial  
20 geomorphology. Significant entrenchment of the fluvial system, followed by aggradation formed  
21 the earliest fluvial terrace (T1), which encompasses environments spanning the transition from  
22 deglaciation into Greenland Interstadial 1 (GI-1). Incision below T1 began towards the end of GI-  
23 1, with three terraces (T2 – T4) between the abandonment of T1 and the early Holocene (15.0 –  
24 9.2 ka). Climatic shifts, limited vegetation cover/soil development, and peri-/paraglacial landscape  
25 instability conditioned the development of the early postglacial fluvial landsystem. Three further  
26 terraces (T5 – T7) developed during the mid- to Late Holocene (6.6 – 3.1 ka), and comprise most  
27 of the valley floor. Climatic instability, glacial inheritance, and widespread anthropogenic

28 disturbances are reflected in greater hillslope-channel coupling during this period. The extent of  
29 later Holocene terraces (T8 – T9) is limited as the river became isolated from flanking hillslopes  
30 entrenched between existing river terraces. Fluvial landscape evolution in formerly glaciated  
31 catchments is strongly conditioned by the cold stage legacy that introduced excess sediment and  
32 landscape instability into the catchment. Subsequent catchment-wide responses are variable and  
33 non-linear, with valley floors operating in a series of reach-wide responses. There is a need for  
34 greater chronological control to constrain the Lateglacial and Holocene evolution in the Tyne  
35 catchment, but also to further our understanding of region-wide responses to external drivers and  
36 local dynamics.

37

38 **Abbreviations:** BIIS, British-Irish Ice Stream; BSW, Bog Surface Wetness; CAM, Central Age  
39 Model; DEM, Digital Elevation Model; GI, Greenland Interstadial; GI, Greenland Stadial; LGM,  
40 Last Glacial Maximum; LiDAR, Light Detection and Ranging; MAM, Minimum Age Model; MIS,  
41 Marine Isotope Stage; NSL, North Sea Lobe; OD, Ordnance Datum; OSL, Optically Stimulated  
42 Luminescence; SAR, Single aliquot regeneration; TGIS, Tyne Gap Ice Stream; YDS, Younger  
43 Dryas Stadial.

44

45 **Keywords:** Lateglacial; Fluvial development; Glacial legacy; Climatic shifts; Tyne valley

46

47 Correspondence to: Lynda Yorke email: [l.yorke@bangor.ac.uk](mailto:l.yorke@bangor.ac.uk)

## 48 1. Introduction

49 River terraces and their deposits are important archives of terrestrial environmental change and  
50 catchment sediment dynamics, as such they can reveal the response of fluvial systems to  
51 external forcing (e.g. climate and extreme events; base-level change; vegetation and land cover;  
52 and, anthropogenic activities) and internal fluvial dynamics. The degree of fluvial response to  
53 driving forces is often linked to landscape and river sensitivity (cf. Brunnsden and Thornes, 1979;  
54 Fryirs, 2017), with sediment availability a major driver of geomorphic change. Changes in  
55 sediment flux can result in channel incision/aggradation, floodplain aggradation, and lateral

56 channel migration. Additionally, local fluvial dynamics and discontinuities between and within  
57 reaches can mute or amplify the response to external drivers (Chiverrell et al., 2010; Philips,  
58 2010). However, compared to other European river systems, the timescales and responses of  
59 British rivers, within the limits of the British-Irish Ice Sheet (BIIS; MIS 2), during the Lateglacial  
60 and early Holocene are poorly constrained, especially in contrast to lowland systems that lay  
61 beyond the BIIS (Collins et al., 2006; Gao et al., 2007; Lewin and Gibbard, 2010; Brown et al.,  
62 2013). Accurately dated fluvial landform sequences in the uplands and piedmont zones of  
63 systems within the MIS 2 ice sheet limit are rare in the UK for this period (Macklin and Lewin,  
64 1993; Macklin et al., 2014), making it difficult to explore potential relationships between fluvial  
65 dynamics and forcing factors. Some important exceptions are available from northern Britain,  
66 however. There are dated sequences from both the eastern and western Pennine rivers such as  
67 the Wharfe (Howard et al., 2000a), Swale (Taylor et al., 2000) and Ure (Howard et al., 2000b;  
68 Bridgland et al., 2011), Hodder and Ribble (Chiverrell et al., 2009a; Foster et al., 2009) and, in  
69 Scotland the Kelvin, Feshie and Spey (Tipping et al., 2008; Ballantyne, 2019; Werritty, 2021).

70

71 Conceptual models of responses of fluvial systems through glacial-interglacial cycles in Northwest  
72 Europe indicate channel instability and channel pattern change, followed by aggradation and  
73 stability (Vandenberghe, 2008; Kaiser et al., 2012). In the UK, transitions from cold-to-warm have  
74 typically been associated with channel incision and erosion, coupled with shifts from a braided  
75 river system to a meandering river system (e.g. Maizels, 1982; Bridgland, 2000; Chiverrell et al.,  
76 2009a; Macklin et al., 2013). Short-lived climatic oscillations (warm-to-cold), such as the Bølling-  
77 Allerød to Younger Dryas, have been recorded as catchment instability and aggradational  
78 episodes in lowland systems (Hill et al., 2008; Howard et al., 2011). The transition from the BIIS  
79 (MIS 2) glacial land-system to post-glacial fluvial system encompassed the climatic changes in  
80 the late glacial (GI-1 and GS-1) and the early Holocene climate events (Mayewski et al., 2004;  
81 Lowe et al., 2008; Lang et al., 2010; Shakun and Carlson, 2010; Thornalley et al., 2009;  
82 Rasmussen et al., 2014). The transition into the early Holocene in northern England was also  
83 accompanied by base-level changes, linked to lower than present sea levels (Bradley et al., 2011;

84 Shennan et al., 2012) and glacio-isostatic uplift (Bridgland et al., 2010; Bridgland and Westaway,  
85 2014). The fluvial system changed from glacial to nival-fed (snowmelt) discharge regimes to  
86 temperate systems, and was marked by reductions in sediment availability reflecting both  
87 exhaustion (cf. Church and Ryder, 1972) and landscape stabilisation with vegetation and soil  
88 cover. Thus, a paraglacial landsystem conceptual model (cf. Ballantyne, 2005; Harrison et al.,  
89 2010) describes the post-glacial development of upland formerly glaciated catchments and  
90 describes the evolution of sediment regimes inside the last glacial maximum (LGM) limits. In this  
91 model the postglacial hillslope processes and fluvial systems of Britain are out of phase with  
92 major climatic shifts, thus the redistribution/availability of the sediment is important and may act  
93 as a lead or lag in fluvial development.

94

95 Northern England lies within the limits of MIS 2 ice and many river valleys, including the Tyne, are  
96 infilled with glacial, soliflucted, colluvial and fluvial deposits. Previous workers have investigated  
97 reaches in the Tyne basin during the mid and late Holocene period (e.g. Passmore and Macklin,  
98 1994; Rumsby and Macklin, 1996), but these studies did not concentrate on the Lateglacial–  
99 Holocene transition. Here, we present evidence for fluvial development for a 22 km stretch of the  
100 piedmont middle Tyne valley. Our aims are: (i) to present the alluvial landform record; (ii) to  
101 identify the sequence of valley-floor development; (iii) to interpret the depositional environment  
102 from the sedimentary record; (iv) to establish a chronological framework using optically stimulated  
103 luminescence dating (OSL); (v) to explore the response of the fluvial system to climate change  
104 and other conditioning factors.

## 105 **2. Study area**

### 106 **2.1. The Tyne Basin**

107 The Tyne basin lies in the northeast of England (Fig. 1) and comprises a catchment area of 2,936  
108 km<sup>2</sup>. The Tyne basin (maximum elevation 893 m) comprises two main tributaries; the North Tyne  
109 rises on the Cheviot Hills near the Scottish border and the South Tyne forms on the North  
110 Pennines near the Cumbrian border. These tributaries combine near Hexham (Fig. 1) to form the  
111 River Tyne. The river Tyne is 118 km in length, and reaches the north sea at Tynemouth.

112 Geologically, the basin is underlain by Carboniferous limestone, sandstone, siltstone and  
113 mudstone, along with Silurian greywackes and Devonian sandstones. Andesite outcrops in the  
114 Cheviot Hills, whilst Dolerite is found along the south Tyne. Structurally, the Alston block and  
115 Northumberland fault-trough bound the catchment (Scrutton, 1995; Johnson, 1997). Investigation  
116 focused on the mid-Tyne valley (w-e flowing section), extending as far upstream as the Allen  
117 confluence (South Tyne) and as far downstream as Broomhaugh (Tyne) (Fig. 1). The Tyne valley  
118 comprises wide valley floors (or basins), with occasional narrow sections (or gorges), and the  
119 present day river can be described as a wandering/meandering gravel-bed river.

120

121 During the last glaciation northern England and the Tyne valley were overridden by British-Irish  
122 Ice Sheet (BIIS) (Hughes et al., 2016). Regionally, the ice was around 0.8 km thick at the LGM. A  
123 west-east flowing ice stream (Tyne Gap Ice Stream; TGIS) extended along the Tyne valley  
124 (Smith, 1994; Mills and Holliday, 1998; Livingstone et al., 2012, 2015) and an ice lobe extended  
125 north–south down the North Sea coast (North Sea Lobe; NSL). Constrained by Bayesian  
126 statistical analysis of radiocarbon and cosmogenic ages, retreat of the TGIS had begun by 18.5–  
127 18.3 ka (Livingstone et al., 2012, 2015; Evans et al., 2021; Clark et al., 2022), creating  
128 accommodation space in the mid and lower Tyne valley as it decoupled from the NSL impounding  
129 waters in the Tyne lowlands. In the Tyne valley an extensive pro-glacial drainage system  
130 developed feeding water and sediments towards a large ice-dammed lake (Glacial Lake Wear)  
131 (Smith, 1994; Davies et al., 2009; Yorke et al., 2012; Teasdale, 2013). The NSL had retreated  
132 completely from the east coast by 17–16.5 ka (Roberts et al., 2018; Evans et al., 2021), with ice  
133 retreating to the upland dispersal centres (Lake District) by 17 ka (Davies et al., 2019). Following  
134 deglaciation, regional sea levels were low, lying at -30 m Ordnance Datum (OD) at 12 ka BP  
135 (Bradley et al., 2011). Buried peats within estuarine sediments found in the lower Tyne constrain  
136 early Holocene marine inundation to 8.5 ka cal. BP (Horton et al., 1999a,b). Glacio-isostatic uplift  
137 across Northumberland has declined since deglaciation, with a present-day uplift rate of 0.2–0.8  
138 mm a<sup>-1</sup> south to north respectively (Bradley et al., 2011; Shennan et al., 2012; Bradley et al.,

139 2023). Base-level change for regional river systems, driven by both eustatic and glacio-isostatic  
140 factors, may have influenced fluvial dynamics during the Lateglacial and early Holocene period.  
141

142 This study focuses on three reaches. Zone I is a lowland reach set within ice-disintegration  
143 topography, where narrow valley floor fluvial terraces are preserved on inner meander banks  
144 between the Allen confluence and a knick-point gorge (Newbrough) upstream of Fourstones.  
145 Zone II is a gently meandering reach that straddles the confluence of North and South Tyne, with  
146 terraces preserved on both sides of the valley floor flanked by subglacial features between  
147 Fourstones and Acomb. Zone III is a major alluvial basin (Corbridge) between Hexham and  
148 Broomhaugh (Fig. 1), with extensive valley floor fluvial terraces present set below extensive  
149 glacial outwash deposits.

### 150 **3. Materials and methods**

#### 151 3.1. Geomorphological mapping

152 Mapping of the valley floor features drew on interpretation of Light Detection and Ranging  
153 (LiDAR) digital elevation model (DEM), supplied by the Environment Agency's Geomatics Group.  
154 The LiDAR DEM had a spatial resolution of 1 m<sup>2</sup>, with a vertical accuracy of ~0.15 m. Mapping  
155 was undertaken using the interpretative tools within ArcGIS. Extensive flat areas and linear  
156 depressions reflect and were digitised as river terrace fragments and palaeochannels  
157 respectively. Identification was possible through manipulation of the DEM to produce hill-shaded  
158 surfaces, narrow elevation range shaded DEMs and interval contours. Field mapped data were  
159 used to 'ground-validate' the terrace fragments and palaeochannels interpreted from the LiDAR  
160 DEM at scales of 1: 10,000.

#### 161 3.2. Sedimentological investigations

162 The sediments underlying the mapped terraces were recorded from river-bank exposures and  
163 using closely spaced sediment profiles interpreted from the British Geological Survey (BGS)  
164 online database of borehole logs. Sediment analysis followed a lithofacies approach (Miall, 1988)  
165 and sediments were recorded on the basis of grain size, bed contact and bedding, sorting and

166 texture, sedimentary structures, colour, and sediment body geometry (Jones et al., 1999). Clast  
167 form and provenance was established by clast (>0.05 m) lithological analysis (Bridgland, 1986).  
168 Established fluvial form-process models (Miall, 1996) underpin interpretations of lithofacies and  
169 helped interpretation of the generalised vertical succession.

### 170 3.3. Optically Stimulated Luminescence dating

171 In the absence of *in situ* organic material for radiocarbon dating, to develop a chronology for the  
172 terrace sequence we used Optically Stimulated Luminescence (OSL) dating to target sands within  
173 terraces 1, 4, 5 and 7. Suitable lithofacies that had the greatest potential to have been exposed to  
174 light prior to deposition (cf. Thrasher et al., 2009) were targeted for OSL dating, e.g. overbank and  
175 bar-top sands. Samples were collected (in daylight) by hammering opaque plastic tubes (300 x 50  
176 mm) into cleaned faces. Bulk materials collected within 30 cm of the OSL sample provide  
177 materials for measurement of moisture content and  $\gamma$  dose rate in the laboratory. Sand-sized  
178 quartz (180-255 $\mu$ m or 90-125 $\mu$ m) mineral grains were extracted from the sediment samples using  
179 standard preparation techniques. These included wet sieving, removal of organic matter using  
180 H<sub>2</sub>O<sub>2</sub> (10%), HCl (10%) treatment to remove carbonates, HF (48%) treatment for 60 minutes  
181 followed by an additional etching in H<sub>2</sub>SiF<sub>6</sub> acid for two weeks to dissolve remaining feldspathic  
182 components as well as heavy mineral separation using sodium polytungstate (2.63g cm<sup>-3</sup>). All the  
183 samples were measured as medium sized (4mm diameter) multigrain aliquots mounted on  
184 aluminium discs inside an automated Risø TL/DA15 luminescence reader (Bøtter-Jensen 1997,  
185 2000) using a SAR post-IR blue OSL measurement protocol (Murray and Wintle, 2000; Banerjee  
186 et al., 2001; Wintle and Murray, 2006). Due to the fluvial nature of the sediments and in order to  
187 avoid overestimating the true depositional age of the sediments as a result of incomplete  
188 bleaching of the OSL signal (Murray et al. 1995, Wallinga 2002), the D<sub>e</sub> estimates were calculated  
189 using a Minimum Age Model (Galbraith et al. 1999) within the 'R' statistical programming  
190 language (Kreutzer et al. 2012). Dose rate calculations are based on the concentrations of  
191 radioactive elements (potassium, thorium, uranium and rubidium) within the sediment. These  
192 were derived from elemental analysis performed by Actlabs (Canada) using induced coupled  
193 plasma mass spectroscopy / atomic emission spectroscopy (ICP-MS/AES) and a fusion sample



194 preparation technique. The final OSL age estimates include an additional 2% systematic error to  
195 account for uncertainties in source calibration. Dose rate and age calculations were obtained  
196 using DRAC version 1.2 developed by Durcan et al. (2015). These are based on Aitken (1985)  
197 and incorporated updated grain size attenuation factors of Brennan et al. (1991) and Guerin et al.  
198 (2012), etch depth attenuation factors of Bell (1979), dose rate conversion factors of Guerin et al.  
199 (2011) and an absorption coefficient for the water content. The contribution of cosmic radiation to  
200 the total dose rate was calculated as a function of latitude, altitude, burial depth and average  
201 over-burden density based on data by Prescott and Hutton (1994). The OSL age estimates  
202 (presented as ka: Table 1) include an additional 2% systematic error to account for uncertainties  
203 in source calibration.

## 204 **4. Results**

### 205 4.1. Fluvial geomorphology

206 Across the three zones (Fig. 1) of the mid-Tyne valley, the geomorphology and longitudinal  
207 height-range relationships reveal nine fluvial terraces that lie between 20 and 2 m above present  
208 river level (T1 – T9; highest to lowest) and the modern floodplain (Fig. 2 and Fig. 3). T1, broadly  
209 20 m above the modern river, comprises fragmented surfaces that lie along the valley margins of  
210 the South Tyne system. However, within zone III the surfaces are laterally extensive (Fig. 2c) and  
211 show some continuity with extensive glaci-fluvial/-lacustrine deposits (Yorke, 2008) in terms of  
212 extent, however, they are inset ~10m below the glaciogenic surfaces. T2 lies at 15 m above  
213 modern river level and is restricted to isolated fragments located towards the outer margins of the  
214 valley, with greater lateral extent in the South Tyne upstream of Newbrough Gorge (zone I). It is  
215 present most extensively around the confluence of the North and South Tyne (zone II), and forms  
216 a component of an alluvial fan at Dilston (Fig. 2c). T3, 14 m above modern river level, is laterally  
217 extensive in zone I along the South Tyne above Newbrough Gorge (Fig. 2a), and restricted to  
218 isolated fragments in zones II-III downstream of Newbrough Gorge, and in the area around the  
219 town of Corbridge, hereafter referred to as the Corbridge Basin (Fig. 2b). This upper group of  
220 terraces lack any surface palaeochannel topography and are altitudinally separated by 8 m from

221 the lower terraces T5 – T9. Their elevated, fragmentary and valley margin nature reflects that  
222 they are terrace remnants preserved in less active sectors of the former floodplain, with removal  
223 from the main channel belt during subsequent fluvial erosion and basal incision that generated  
224 terraces T4 – T9.

225

226 T4, at 9 m above current river level, occurs throughout zones I to III, but is most extensive in zone  
227 III, the Corbridge Basin. The terrace long profile shows a reduction in gradient downstream from  
228 0.05 to 0.01, and lies closer in elevation to the present river downstream (9 to 6 m above river  
229 level). Several sinuous (sinuosity index 1.3) palaeochannels are visible on T4 (zone III), indicating  
230 a meandering system and suggesting some lateral stability of channel systems. T5 lies 6 m above  
231 the base of the modern river and has limited presence throughout the study area. T5 grades into  
232 the Newbrough Gorge. Numerous surficial palaeochannels are evident on this terrace, and their  
233 planform sinuosity is almost straight (sinuosity index <1.05). The channels show evidence of  
234 progressive lateral change through avulsion and chute cutoffs. T6 lies 5 m above the bed of the  
235 present river and is present in all zones, I – III. T6 extensively occupies the meander bend within  
236 zone III. Surficial palaeochannels are ubiquitous on this terrace, and whilst sinuosity is straight to  
237 low (sinuosity index <1.05–1.03), in zones II – III channel planforms indicate bar progradation and  
238 downstream translation of the meander bend. Migration within these palaeochannels is similar to  
239 the development of the present-day meanders. T7 is only present in zones I – II, lies 4 m above  
240 the modern river and is sculpted with extensive palaeochannels. Their morphology reflects a low-  
241 sinuosity (sinuosity index 1.06–1.30) planform, with lateral valley-floor channel migration through  
242 avulsion and chute cut-offs.

243

244 T8 and T9 are the least extensive terraces recorded in the main Tyne valley. T8 lies 3 m above  
245 the base of the modern river, and is present in zone II immediately upstream and downstream of  
246 the Tyne confluence. T9 lies 2 m above the present river, occurs as discrete deposits along the  
247 inner banks of the meanders in zone I (Allen Fan), and in zone III associated with the Dilston Fan  
248 (zone III). Both T8 and T9 reflect the most recent depositional activity of the river.

249

250 The South Tyne valley-floor (zones I–II), through to the confluence, is dominated by T6 and T7,  
251 bounded by the higher T1 to T4. T6 and T7 form a significant sediment depocenter (*sensu*  
252 Chiverrell et al., 2010) in the South Tyne accounting for >90% of the valley floor. Zone III  
253 continues to be dominated by T6, accounting for >80% of the valley floor and represents another  
254 significant depocentre. Zone II forms a division, separating the higher T5 of the South Tyne  
255 system from the lower T6 and T7 of the River Tyne. The narrow Newbrough Gorge, South Tyne,  
256 with its lack of valley floor provides a natural break in the terrace sequence.

257

258 Alluvial fans have formed at the mouths of a number of small tributaries but two significant fans  
259 are found at confluences of the River Allen (zone I) and Devil's Water (Dilston Fan, zone III). The  
260 Allen Fan terrace sequence comprises T6 and T7 and is coherent with the terraces in the South  
261 Tyne, and suggests a younger development of this fan. The Dilston Fan terrace sequence  
262 comprises an older sequence of terraces, with T1 to T5 present, with T5 grading into the valley-  
263 floor sequence. The Dilston Fan represents a long history of formation that corresponds with the  
264 Lateglacial and Holocene fluvial development of the Tyne fluvial terraces.

#### 265 4.2. Sediments and geochronology

266 Exposure of the fluvial succession adjacent to the modern channel is restricted to cut-bank  
267 exposures at Fourstones (Zone II) and Farnley Haugh (Zone III) which reveal detail on the  
268 stratigraphy of T1, 4, 5 and 7. Borehole logs (from the BGS archive) provided additional sub-  
269 surface stratigraphy for T1, 6 and 7.

270

##### 271 4.2.1. The A69 (Zone II) and A68 (Zone III) borehole series

272 Borehole logs from the construction of the A69 (near Hexham) and A68 roads (near Broomhaugh)  
273 show the sediment stratigraphy (Fig. 4a,b) extending to bedrock revealing a significant infill of  
274 basal sediments in the Tyne valley (Fig. 5a,b). The profile indicates incision into bedrock to ~10 m  
275 OD and the undulations in the bedrock surface reflect a former channel position. This channel is  
276 offset from the current day river, and has a channel base falling from 0 m OD below zone II to -30

277 m OD near the estuary (Cumming, 1971, 1977). The incision of the bedrock valley probably  
278 reflects some glacial deepening by ice draining the Tyne Gap and North Tyne Valley, and/or  
279 earlier fluvial incision under lower eustatic sea levels (Cox, 1983; Mills and Holliday, 1998). The  
280 channel forms a palaeovalley to the north of the present-day river. The valley sediment fill  
281 comprises basal over-consolidated diamicts ~5 m thick. Moving downstream the palaeovalley  
282 (Fig. 6) the glacial diamict thickens towards the valley centre (~15 m thick), and is overlain by  
283 pro-glacial sands and sandy gravels of varying from 10 to >15 m in thickness (Fig. 5, 6). This  
284 sequence records the presence of ice in the region, and the subsequent ice retreat with the  
285 development of the pro-glacial drainage system (Yorke et al., 2012; Livingstone et al., 2012). The  
286 basal sediments represent >20 m of aggradation and were likely deposited between 30 and 15 ka  
287 BP (Livingstone et al., 2015). The upper bounding surface of these glacigenic sediments forms a  
288 base to the overlying post-glacial fluvial succession.

289

290 The A68 borehole series crosses the valley-floor, revealing the composition of T1 and T4 (Fig. 4b,  
291 5b). T4 shows incision to a diamict surface, and subsequent aggradation of ~6 m of sandy  
292 gravels, overlain by ~10 m of silty, gravelly sands and capped by 1-2 m of silty sands. The  
293 sedimentary sequence and palaeochannels visible on the surface of T4 suggest a meandering  
294 fluvial system. The A69 borehole series crosses both T6 and T7 (Fig. 4a, 5a) recording for T6 a  
295 basal post-glacial unit of ~7 m thick sandy gravels, with occasional silty sands. Towards the outer  
296 margins of the valley within T6 there are three discrete units cut into the sandy gravels. These  
297 units comprise a channel fill of <2 m laminated peat and peaty silt, and the whole sequence is  
298 buried by 4 m of laminated silts. Well-developed meanders and scroll-bar forms on T6  
299 downstream of Newbrough Gorge (zone II) identify lateral migration of the channel reflecting  
300 increased sediment mobility and stream power. Meandering and migration of scroll-bars has led  
301 to development of 'peaty' back-channel swamp environments with channel migration (Hooke,  
302 2003, 2004; van de Lageweg et al., 2014). For T7, ~7 m of sandy gravels overlie the diamict,  
303 capped by ~1 m of laminated silty sands. Both the T6 and T7 sequences suggest a transition  
304 from a high-energy channel to a low-energy system. The sandy gravels reflect bedload deposition

305 within the main channel, with the silty sands indicative of overbank deposition. The silty sands of  
306 T7 exposed at Fourstones and were targeted for OSL dating (X2733) to constrain the meandering  
307 and scroll-bar progradation associated with T6 – T7.

308

#### 309 4.2.2. Exposures at Farnley Haughs

310 Near Farnley Haughs (zone III) a 20 m long erosion scar (Fig. 6a) exposes the sediments  
311 comprising T1. Thinly laminated, very fine basal sands are interpreted as subaqueous glacio-  
312 fluvial sediments (Yorke et al., 2012). High elevation valley-side glacial outwash terraces reflect a  
313 proglacial drainage system entering Glacial Lake Wear, dammed by the NSL to the east (Smith,  
314 1994; Yorke et al., 2012; Davies et al., 2019). This unit is overlain unconformably by ~4 m of  
315 fluvial sediments comprising rounded cobbles, forming a concave channel lag deposit at the base  
316 of the post-glacial sequence. Above the channel lag are rounded, clast- to matrix-supported  
317 gravels (predominantly Carboniferous sandstones and greywacke, and igneous clasts inc. Shap  
318 granite originating from the Lake District), which reflect vertical accretion as longitudinal bars, with  
319 initial aggradation in low water from tractional processes and small-scale structures  
320 superimposed on the larger bedforms during waning flow (Miall, 1996; Bridge, 2009; Rice et al.,  
321 2009). The longitudinal bars are intercalated with coarse sandy gravel, pebbly sands and silty  
322 sands, which indicates fluctuating flows (Smith et al., 2009; Rice and Church, 2010) (Fig. 6b).  
323 Laminated fine sands (2 m thickness), indicative of overbank deposition, cap the sequence and  
324 are typical of floodplains adjacent to shallow, wandering gravel-bed river (Miall, 1996). The upper  
325 sands were sampled for OSL dating (X2734; Fig. 6b) to constrain late-stage aggradation of T1  
326 and provide a younger than constraint on the incision to T2.

327

#### 328 4.2.3. Exposures at Fourstones

329 T4 and T5 were examined through a cut-bank section that exposes 0.5 km of sediments, opposite  
330 the town of Fourstones (zone II) (Fig. 7a). For T4, the section reveals a basal till (which forms the  
331 stream bed), overlain by ~4 m of well-rounded, weakly horizontal-stratified to structureless  
332 cobble- and boulder-rich gravels (a-axis up to 120 cm) that are indurated with iron-manganese

333 coatings and imbrication is well developed. Clasts within T4 are predominantly volcanic and  
334 igneous in origin (81%), with fewer Carboniferous sandstones, limestones and mudstones (19%).  
335 This matches the clast lithologies recorded within the till (predominantly Lake District volcanic and  
336 igneous clasts – dolerite, quartzite and granite, with subordinate amounts of Carboniferous  
337 sedimentary clasts), indicating that the river reworked earlier sequences. A chute channel  
338 truncates the gravel at the downstream end of T4, and is infilled with cross-stratified to massive  
339 cobble- and pebble-sized sandy gravel, indicative of high relief bar edges, overlain by laminated  
340 sands. Chronological control for T4 was obtained from the laminated sands (X2730) (Fig. 7b).  
341 The stratified gravels represent bedload, with sorting, imbrication and iron-coatings all indicate  
342 transport and deposition in shallow water/fluctuating water levels. The presence of large boulders,  
343 structureless gravels, chute channel and bar deposits in the upper 2 m suggests higher-  
344 magnitude flows (Desloges and Church 1987; Smith, 1990; Brierley and Hickin, 1991). The  
345 sequence is interpreted as a wandering gravel-bed system (Miall, 1996), with periods of lateral  
346 channel instability during extreme flow events (Wooldridge and Hicken, 2005).

347

348 For T5, the sequence displayed extensive exposure of the basal lodgement till (~2 m). The fluvial  
349 sediments of T5 appear to reflect a large remnant palaeochannel, channel bed deposits and  
350 occasional infilled chute channels. The palaeochannel sediments form the boundary between T4  
351 and 5, comprising ~4 m of laminated to massive sands, overlain by a silty sandy clay, with  
352 intercalated sandy gravel layers (Fig. 7b). The sands were sampled for OSL dating (X2731;  
353 X2732). The basal sands probably formed under upper flow regime conditions (Smith, 1990;  
354 Tucker, 2011), with the overlying sandy clays and intercalated gravels suggesting slower flows  
355 with occasional fluctuations in stream competence (Miall, 1996; Bridge, 2009). The sands grade  
356 (downstream) into a sequence of horizontally bedded gravel, with intercalated sands (~6 m thick),  
357 capped by laminated sands (~1 m thick). The gravels comprised 47% volcanic and igneous  
358 clasts, with 52% Carboniferous sandstones and mudstones, and sub-ordinate amounts of coal.  
359 The gravel geometry suggests development of longitudinal bars in shallow water, (Whiting et al.,  
360 1988; Miall, 1996). Periods of lateral instability and high-energy flows are indicated by the multi-

361 storey layers of inversely graded clast- to matrix-supported cobble- and pebble-sized gravel, and  
362 thinly laminated sands, cut into the sands. Within the gravels, chute channels are infilled with  
363 laminated silty clays and suggest channel migration and abandonment, with deposition under  
364 slack water conditions (Smith, 1990; Miall, 1996). The silty clays provided an opportunity for OSL  
365 dating T5 (X2832). The sequence represents the main channel belt, with deposition towards the  
366 outer margins of the valley floor, and is typical of a wandering gravel bed system (Miall, 1996).

367

#### 368 4.3. Geochronology and fluvial sequence

369 The new geochronological control obtained for T1, 4, 5 and 7 of the Tyne sequence, alongside  
370 two existing  $^{14}\text{C}$  ages of  $5900 \pm 70$  cal. BP (BETA-37060) for T5 (tree trunk in basal gravels) at  
371 Farnley Haughs (Passmore and Macklin, 1994) and  $3030 \pm 60$  cal. BP (BETA-45549) for T7 (wood  
372 fragments within a basal channel incised into till) at Lambley (Fig. 1, ~13km upstream of the Allen  
373 confluence; Passmore and Macklin, 2000) provide a basis for exploring the landform sequence.  
374 We discounted Passmore and Macklin's (1994) OSL age of  $2.45 \pm 3.5$  ka obtained from T5  
375 (upper sequence channel fill sandy silts) at Farnley Haughs on the basis that it was obtained 30  
376 years ago. Significant improvements in techniques and instrumentation in the last 20 years have  
377 occurred and it was not until post-1999 that OSL dating protocols became more reliable (Wintle,  
378 2008; Mahan et al., 2022). We have employed an approach, using OxCal (Bronk Ramsey, 2001),  
379 that facilitates statistical testing of these theoretical models of the likely relative order of events in  
380 the Tyne geomorphology (Chiverrell et al., 2009b). Bayesian assessment using OxCal of these  
381 relative order models (Bronk Ramsey, 2008) helps with identification (Fig. 8) of anomalous ages  
382 that are nonconformable and/or out of sequence (Buck et al., 1996; Chiverrell et al., 2009b). The  
383 objective with the dating was to constrain the timing of switches between river terrace levels, but  
384 these are rarely dated directly, typically sitting as erosion episodes between landforms and  
385 derived ages. The Bayesian models were coded in OxCal v4.4.4 Bronk Ramsey (2021) and using  
386 the INTCAL20 atmospheric data from Reimer et al. (2020) as a Sequence model. The Prior  
387 models in Bayesian nomenclature are structured as a series of Phases, which are unordered  
388 groups of events/parameters that contain age information e.g. the differing individual river

389 terraces. Boundaries, in the OxCal nomenclature, use the relationships between dated individual  
390 samples or Phases to generate estimated age probability ranges for undated events (e.g., T1 to  
391 T4 Boundary in Fig. 7). The Tyne model (Fig. 8) has an overall agreement index of 90%  
392 exceeding the >60% threshold advocated by Bronk Ramsey (2009). This level of agreement was  
393 achieved by handling three OSL ages as 100% outliers as detailed below.

394

395 OSL ages obtained from overbank sands at Fourstones (zone II) and Farnley (zone III) (Table 1)  
396 alongside the published  $^{14}\text{C}$  age (tree trunk within basal gravels of our T4; Passmore and Macklin,  
397 1994) help to establish an outline geochronological framework for the Tyne terraces. The  
398 uppermost alluvial sediments of T1 (Farnley) provided an OSL age (X2734) of  $12.9 \pm 1$  ka (Fig.  
399 9a). T2 and T3 remained undated, but the top of the T4 (Fourstones) sequence yielded an OSL  
400 age (X2730) of  $10.7 \pm 1.1$  ka (Fig. 9b). Samples from T5 (X2731; X2732; X2832) returned OSL  
401 ages suggestive of poor resetting of the OSL signal and were regarded on that basis as too old.  
402 The uppermost sediments of T7 (Fourstones) yielded an OSL age (X2733) of  $3.2 \pm 0.5$  ka (Fig.  
403 9c). Though not dated here historic map data suggest that T8 and T9 relate to the last 300 years.  
404 The OSL ages obtained suggest the major terraces developed during the Lateglacial to mid-  
405 Holocene period. The Bayesian modelling has calculated modelled age probability distributions  
406 for the evolution of the Tyne terraces, constraining the T1 / Deglacial transition to  $16.0 \pm 2.1$  ka,  
407 the progression from T1 to T4 to  $11.9 \pm 2.7$  ka, T4 to T5 to  $8.7 \pm 2.3$  ka, and T5 to T7  $4.0 \pm 1.8$  ka.  
408

## 409 **5. Discussion**

### 410 **5.1. Late MIS 2 to GI-1**

411 In northern Britain, landscape development with deglaciation responded to the progressive retreat  
412 of the TGIS, with regional ice retreat models indicating that the Tyne valley deglaciated before  
413 16.4–15.7 ka during a regional collapse of ice dispersal centres. As changes to ice drainage  
414 routeways developed with deglaciation more local topographical control of ice became dominant  
415 (Hughes et al., 2014; Livingstone et al., 2015; Davies et al., 2019). An extensive proglacial



416 drainage network developed in the Tyne draining towards Glacial Lake Wear (Yorke et al., 2012),  
417 which formed between 17.0 and 16.5 ka as the NSL extended across the lowlands impounding  
418 glacial meltwaters (Smith, 1994; Bateman et al., 2011; Davies et al., 2019). Ice marginal  
419 glaciofluvial and glaciolacustrine sediments aggraded against the retreating and decaying Tyne  
420 Gap Ice Stream, forming a series of valley side outwash terraces (Peel, 1941; Mills and Halliday,  
421 1998; Yorke, 2008; Livingston et al., 2015). The highest outwash deposits lie at between 30 and  
422 40 m above the base of the present river, and likely aggraded during the period  $16.0 \pm 2.1$  ka.

423

424 The earliest of the Tyne fluvial terraces (T1) are inset 10 m below the lowest outwash surface. An  
425 OSL age (X2734) obtained from the overbank sands of T1 dates indicates fluvial aggradation up  
426 to  $12.9 \pm 1$  ka and implies the river was active during the Interstadial (GI-1). T1 comprises coarse  
427 gravels, intercalated with sandy layers and capped by fine silty sands, typical of channel and bar  
428 features and material deposited from overbank flows. The fluvial system is considered to be  
429 meandering, with episodic flooding events and intermittent fluvial-lacustrine conditions (Gibbard  
430 and Lewin, 2002), possibly developing during the earliest phase (GI-1e/d) before the landscape  
431 stabilised and vegetation cover (i.e. *Betula*, *Juniperus*) became established (Innes et al., 2021).  
432 The upper part of the unit represents repeated overbank deposition and suggests the channel  
433 had already begun to incise or laterally migrate during the latter stages of the Interstadial, with  
434 this area of active channel replaced by floodplain aggradation (Vandenberghe, 2015).

435

## 436 5.2. GS-1 to early Holocene

437 Between the onset of GS-1 and the early Holocene, the OSL ages obtained from T1 and T4 ( $12.9$   
438  $\pm 1$  ka and  $10.7 \pm 1$  ka) imply cycles of fluvial incision and aggradation characterised the  
439 transitional phase of the Lateglacial period. The event boundary creates a timeframe of 13.3 to  
440 10.4 ka for the development of this upper group of terraces. Cooling at the transition between GI-  
441 1a and GS-1 signified a return to cold stage conditions (Bakke et al., 2009). The partially wooded  
442 conditions established during GI-1 were impacted by the periglacial conditions, with open

443 woodland and shrub-heath replaced by sedge-tundra open herbaceous vegetation (Innes, 1999;  
444 Innes et al., 2021).

445

446 The absence of accessible sediments prevents an interpretation of T2 and T3, however, T2  
447 represents incision and aggradation after 12.9 ka. If we assume they are cut and fill rather than  
448 erosional terraces (Lewin and Macklin, 2003 suggest renewed aggradation during GI-1) then their  
449 development can be linked to hydrological and landscape change during GI-1. We infer that  
450 geomorphic activity was strongly conditioned by periglacial slope processes and paraglacial  
451 adjustment during GI-1 (Chiverrell et al., 2007; Passmore and Waddington, 2009; Ballantyne,  
452 2019; Harrison et al., 2021), driven by nival flow and spring flood runoff, creating a sediment-  
453 dominated fluvial system. T4 returned an OSL age of  $10.7 \pm 1$  ka (X2730; obtained from the  
454 upper sands) implying aggradation during the earliest Holocene and that incision or channel  
455 abandonment had probably already occurred as overbank sedimentation had begun. If we  
456 assume that sediment exhaustion has not occurred by the early Holocene, and with shifts to  
457 cooler, wetter conditions at 11.2, 11.4 and 10.8 ka cal. BP (Barber et al., 2003; Mayewski et al.,  
458 2004; Lang et al., 2010; Vincent et al., 2011) recorded in terrestrial, lacustrine and bog surface  
459 wetness (BSW) records, it is easy to envisage a situation where paraglacial adjustment remained  
460 dominant (Ballantyne, 2005; 2019) and a sediment-dominated fluvial system persisted. The  
461 presence of this higher group of terraces (T1-T4) and the Dilston fan (Zone I) suggests the period  
462 was dynamic and unstable and that cycles of incision and aggradation during the GS-1 continued  
463 into early Holocene period. Comparable responses are evident from the landform sequences of  
464 river systems in north Northumberland, the Southern Uplands, central Scotland and the Highlands  
465 (Tipping et al., 2008; Passmore and Waddington, 2009, Ballantyne, 2019; Werritty, 2021).

### 466 5.3. Early to Mid-Holocene

467 Early to mid-Holocene fluvial development is reflected in a single incision and aggradation cycle,  
468 leading to the development of T4 and T5. The incision of T4 occurred after  $10.7 \pm 1$  ka (X2730).  
469 Although OSL ages were obtained for T5 (X2731, X2732, X2832) the model identified these as  
470 outliers and were disregarded. The rationale for this was that the obtained OSL ages were too old

471 and were most likely the result of poor resetting of the OSL signal. Thus, development of T4 and  
472 T5 is constrained to the period  $8.7 \pm 2.3$  ka (probability-based time frame). Both T4 and T5 have  
473 low sinuosity to straight palaeochannels evident on their surfaces, and the sediments comprise  
474 lithofacies assemblages of crudely bedded, imbricated coarse sandy gravels, overlain by a  
475 veneer of silty sands. Channel fills within the sequence comprise poorly bedded sands, silty  
476 sands and silts, with occasional lenses of coarse boulders and inversely graded sands, thought to  
477 represent flooding events. The sediments of T4 and T5 are interpreted as channel bed and bar  
478 deposits, channel fills and overbank sedimentation. T4 sequences suggest low aggradation rates  
479 and laterally stable channels during the early Holocene, whereas T5 comprises some vertically  
480 stacked sequences suggesting periods of instability as we moved towards the mid-Holocene. The  
481 early to mid-Holocene landscape was one of increasing stability and soil development, with  
482 regional vegetation records indicating that open grasslands and shrubs were replaced by  
483 postglacial woodlands (*Juniperus*, *Betula* and *Corylus*) (Innes, 1999; Vincent et al., 2011; Ghilardi  
484 and O'Connell, 2013; Innes et al., 2021). Anthropogenic disturbances have been recorded in  
485 North Tyne pollen sequences (Moores, 1998) as early as 8.5 ka BP (late Mesolithic), which when  
486 combined with recorded cooler and wetter conditions at 8.6–8.2 and 7.8–7.4 ka cal. BP (Barber et  
487 al., 2003; Lang et al., 2010; Vincent et al., 2011) may explain the flooding deposits and lateral  
488 instability recorded as we move towards the mid-Holocene.

#### 489 5.4. Mid to Late Holocene

490 The mid- to Late Holocene fluvial development is reflected in the lower group of terraces, T5 to  
491 T7. An OSL age of  $3.2 \pm 0.5$  ka (X2733) was obtained from overbank sands of T7, and  
492 development of T5 – T7 has been constrained to  $4.0 \pm 1.8$  ka (probability-based time frame). T6  
493 and T7 dominate zones II and III, however, only T6 is present in zone I and inset below the higher  
494 terrace group (T1-T4) and the outwash terraces. Palaeochannels on the surface of T6 indicate  
495 low to moderately sinuous channels suggesting development of a wandering-gravel bed system,  
496 however, there are several migratory meander bends, evidenced by scroll-bars, indicating  
497 channel instability. The sediments of T6 and T7 comprise basal sandy gravels that pass into silty  
498 sands and laminated silts. Significant peat-infilled channels and silty peats dominate the upper

499 lithofacies assemblages. These suggest laterally migrating channels, and backwater zones are  
500 indicated by the burial of peat-filled channels and slough channels infilled with inverted  
501 stratigraphy towards the outer margins of T6. During this period, climatic instability is reflected in  
502 increased bog surface wetness (BSW) records at 6.2, 5.7, 5.4, 5.4, 4.4–4.0 ka cal. BP (Hughes et al.,  
503 al., 2000; Barber et al., 2003; Charman et al., 2006). Additionally, regional vegetation records  
504 (Moores, 1998; Moores et al., 1999) indicate early anthropogenic disturbances in the North Tyne  
505 catchment, with significant human activity from the late Mesolithic through to the Neolithic (*cf.*  
506 Tolan-Smith, 1996; Waddington and Passmore, 2009). The landscape became largely tree-less,  
507 with cultivated pollen taxa and anthropogenic indicator species dominating, especially during the  
508 late Bronze Age to Romano-British period. It is easy to envisage periods of widespread fluvial  
509 activity driven by increased incidence of flooding, extreme events and channel abandonment in a  
510 landscape that was primed (sensitised) by human disturbances and with a paraglacial legacy  
511 (Ballantyne, 2005; 2019) providing plentiful erodible sediments. The extent of T6 and T7 (Zones I-  
512 III), including the Allen fan (Zone III) reflect major fluvial activity within the catchment, with  
513 significant valley floor reworking and probable reincorporation of earlier fluvial deposits but it did  
514 not incise into its Lateglacial valley infill (Figs. 5 & 6).

515

516 Passmore and Macklin (2000) present a radiocarbon date of 3.2 ka cal. BP (BETA-45549) for (our)  
517 T7, obtained from the South Tyne at Lambley (Fig. 1), however, Passmore and Macklin (1994)  
518 also present a radiocarbon date of 5.7 ka cal. BP for (our) T4 and an OSL age of  $2.45 \pm 3.5$  ka for  
519 (our) T5, obtained from the Tyne at Farnley Haughs (though discounted for the Bayesian model  
520 due to reliability of OSL ages obtained using earlier dating protocols) that raises questions about  
521 our chronology. However, there is very little altitudinal separation between T5 and T7 (only 2m),  
522 and the terrace long profile (Fig. 3) shows that the surfaces lie closer in elevation downstream  
523 and may reflect lateral variability evidenced by the switch to scroll-bars on the surface of T6,  
524 rather than significant incision. In addition, sediment deposition at Farnley Haughs occurs in a  
525 pinch-point in the valley, potentially allowing higher aggradation at this site compared to the open  
526 valley floor setting in the South Tyne at Lambley and Fourstones. Whilst significant

527 improvements in dating protocols (both radiocarbon and OSL) have occurred in the last 30 years  
528 (Wintle, 2008; Mahan et al., 2022), we could be seeing a situation of pass-the-parcel sediment  
529 movement through depocentres (*sensu* Chiverrell et al., 2010) and a well-ordered younging  
530 progression downstream is not present. Using an example from the last 200 years, Passmore and  
531 Macklin (2000) have shown that in response to 18<sup>th</sup> Century metal mining-induced sedimentation  
532 and Little Ice Age (LIA) climatic instability the Tyne propagated sediment slugs (*cf.* Nicholas et al.,  
533 1995) through its system. The widespread lateral instability in the uplands was subsequently  
534 transmitted downstream in a time-transgressive manner.

535

536 The last 3 ka has seen periods of increased instability recorded in river systems throughout  
537 northern England (Foster et al., 2009; Chiverrell et al, 2010; Macklin et al., 2014). The results  
538 here suggest that there is limited later Holocene activity in the central reaches of the Tyne Valley.  
539 Although T8 and T9 are undated, they must be younger than  $3.2 \pm 0.5$  ka based on the OSL age  
540 obtained from T7 (X2734). They constitute the least well-developed terraces in the sequence due  
541 to their limited extent along the central reaches. Comparable to those recorded in the South Tyne  
542 at Lambley (Passmore and Macklin, 2000), they most likely developed during the recent historic  
543 period. Early clearance of the Tyne catchment likely explains regional (northern England)  
544 variations in fluvial response during this period, driven by the relationship between land-use  
545 changes, climatic shifts and flooding episodes. Whilst incision (down to bedrock) is recorded in  
546 the tributaries of the South Tyne during last 1.2 ka (Macklin et al., 1992), it appears that there is a  
547 disconnect between the uplands (hillslope) and channel after the large depocentres (T6 – T7)  
548 developed, and subsequent periods of instability were reflected in lateral channel migration and  
549 reach instability, but not in further cut and fill episodes in the central reaches.

550

551 Naturally, the uplands with their connectivity to hillslopes and their fragility in terms of land cover  
552 would be more sensitive to external forcing. The response to such forcing is evident in the  
553 channel floor activity and incision seen in the upper reaches of the South and North Tyne rivers  
554 and their tributaries (Macklin et al., 1992; Moores et al., 1999; Passmore and Macklin, 2000;

555 Macklin and Rumsby, 2007). The fluvial response in the uplands (South Tyne tributaries) has  
556 been much more dynamic and sensitive to climatic instabilities and anthropogenic activity  
557 (Macklin et al., 1992; Rumsby and Macklin, 1996) during the last 1 ka than that in the central  
558 zones in the Tyne Valley corridor, which have been relatively stable since the onset of the later  
559 Holocene period. This indicates that major sub-sections of the catchment are not synchronous.  
560 Therefore, the upper catchment can be assumed to be more sensitive to change, and that  
561 connectivity between the hillslope and the catchment is weaker in the piedmont zone. This  
562 suggests that catchment-wide response is diachronous, and it is apparent that the system is  
563 operating in discrete, reach-wide responses, such that correlating terraces throughout the whole  
564 system is not always possible.

## 565 **6. Conclusion**

566 This study aimed to reconstruct the alluvial record of the Tyne valley following deglaciation.  
567 Through a combination of geomorphological mapping and sedimentological investigations,  
568 combined with new OSL ages obtained from fluvial sands, we have been able to present a valley  
569 floor history that spans the period following retreat of the TGIS up to the recent historic period.  
570

571 The Tyne valley terrace sequence reveals significant alluvial response following deglaciation,  
572 resulting in a pattern of incision and valley refilling and leading to the presence of nine alluvial  
573 terraces lying between 20 and 2 m (T1 – T9) above present river level. New OSL ages obtained  
574 from T1 ( $12.9 \pm 1$  ka), T4 ( $10.7 \pm 1$  ka) and T7 ( $3.2 \pm 0.5$  ka), alongside probability-based modelling  
575 bracket terrace development to four phases (i) deglacial phase:  $16.0 \pm 2.1$  ka; proglacial outwash  
576 terraces, (ii) Lateglacial phase:  $11.9 \pm 3.1$  ka; high level alluvial terraces T1-T4, (iii) early to mid-  
577 Holocene phase:  $8.7 \pm 2.3$  ka; alluvial terraces T4-T5, and (iv) mid- to late Holocene phase:  $4.0 \pm$   
578  $1.8$  ka; low level extensive alluvial terraces T5-T7. The later Holocene to recent historic period is  
579 reflected by the presence of T8 and T9.

580

581 Development of T1 to T4 was in response to climatic shifts (GI-1, GS-1, and early Holocene  
582 events), associated landscape instability and the legacy of glacial inheritance during GS-1 and

583 early Holocene. This is in contrast with previous studies that suggested there was little/no activity  
584 during the early Holocene. However, we suggest this was, in part, due to a lack of dated  
585 sequences and the lack of high-resolution digital terrain (LiDAR) data to facilitate better  
586 identification.

587

588 Significant fluvial activity is recorded during the mid- to late Holocene, with T6 and T7  
589 representing a major period of landscape instability and reorganisation. These laterally extensive  
590 terraces comprise most of the valley floor sequence, and reflect a period of upland landscape  
591 stripping and redistribution driven by increased precipitation due to climatic instability, major  
592 anthropogenic disturbances, and a ready supply of easily erodible glacial sediments.  
593 Subsequent fluvial activity suggests cannibalisation of earlier terraces, with recent historic activity  
594 (T8 and T9) confined to within these dominant terraces (T6 – T7).

595

596 The sedimentary sequence underlying the terraces indicates that incision following deglaciation  
597 did not incised through the glacial infill (in the mid-Tyne valley) and there is a clear boundary  
598 between those sediments and the Holocene fill. The sediments underlying the terraces reflect  
599 transition from a meandering system during the early postglacial phase to a dominant wandering-  
600 gravel bed system that persists today.

601

602 This research highlights the importance of catchment-wide investigations and the need for  
603 rigorous dating controls. The Tyne valley terrace sequence reflects the importance of complex  
604 responses within the fluvial system, and demonstrates that localised responses can temper and  
605 impact the broader responses to external climatic drivers. The results are broadly similar to  
606 models of fluvial response in other upland UK (Chiverrell et al., 2010) and northern European  
607 systems (Vandenderge 2008, 2015) but highlights that the valley floor has been operating in a  
608 series of discrete reach-wide responses, and thus, correlation of terraces throughout the whole  
609 system is not always possible.

610

611 **Acknowledgements**

612 This paper is based upon work undertaken when LY was in receipt of a University of Hull PhD  
613 Scholarship. The two anonymous reviewers are thanked for their positive and constructive  
614 comments. OSL dating work was funded by a joint Quaternary Research Association (QRA) and  
615 Research Laboratory for Archaeology and History of Art (University of Oxford) Luminescence  
616 Dating Award given to LY. We thank the numerous landowners along the Tyne valley for granting  
617 access to their land, and CEMEX for access to their quarry sites. LY would like to thank Dr  
618 Barbara Rumsby for the continued support and advice over the years. We thank our colleagues  
619 for their valuable time, contributions to fieldwork and useful discussions.



620 **References**

- 621 Aitken, M.J., 1985. Thermoluminescence dating: past progress and future trends. *Nuclear Tracks*  
622 *and Radiation Measurements* (1982) 10(1–2), 3–6. [https://doi.org/10.1016/0735-](https://doi.org/10.1016/0735-245X(85)90003-1)  
623 [245X\(85\)90003-1](https://doi.org/10.1016/0735-245X(85)90003-1)
- 624 Bakke, J., Lie, Ø., Heegaard, E., Dokken, T., Haug, G.H., Birks, H.H., Dulski, P., Nilsen, T., 2009.  
625 Rapid oceanic and atmospheric changes during the Younger Dryas cold period. *Nature*  
626 *Geoscience* 2, 202–205. <https://doi.org/10.1038/ngeo439>
- 627 Ballantyne, C.K., 2005. Paraglacial Landsystems. In: Evans, D.J.A. (Ed.), *Glacial Landsystems*.  
628 Hodder Arnold, London, pp. 432–461.
- 629 Ballantyne, C.K., 2019. After the ice: Lateglacial and Holocene landforms and landscape  
630 evolution in Scotland. *Earth and Environmental Science Transactions of the Royal Society*  
631 *of Edinburgh* 110(1–2), 33–171. <https://doi.org/10.1017/S175569101800004X>
- 632 Banerjee, D., Murray, A.S., Bøtter-Jensen, L., Lang, A., 2001. Equivalent dose estimation using a  
633 single aliquot of polymineral fine grains. *Radiation measurements* 33(1), 73–94.  
634 [https://doi.org/10.1016/S1350-4487\(00\)00101-3](https://doi.org/10.1016/S1350-4487(00)00101-3)
- 635 Barber, K.E., Chambers, F.M., Maddy, D., 2003. Holocene palaeoclimates from peat stratigraphy:  
636 macrofossil proxy climate records from three oceanic raised bogs in England and Ireland.  
637 *Quaternary Science Reviews* 22, 521–539. <https://doi.org/10.1016/S0277-3791>
- 638 Bateman, M.D., Buckland, P.C., Whyte, M.A., Ashurst, R.A., Boulter, C., Panagiotakopulu, E.,  
639 2011. Re-evaluation of the Last Glacial Maximum typesite at Dimlington, UK. *Boreas* 40,  
640 573–584. <https://doi.org/10.1111/j.1502-3885>
- 641 Bell, W.T., 1979 Attenuation factors for the absorbed radiation dose in quartz inclusions for  
642 thermoluminescence dating. *Ancient TL* 8, 1–12.
- 643 Bendle, J.M., Glasser, N.F., 2012. Palaeoclimatic reconstruction from lateglacial (younger dryas  
644 chronozone) cirque glaciers in snowdonia, north wales. *Proceedings of the Geologists'*  
645 *Association* 123(1), 130–145. <https://doi.org/10.1016/j.pgeola.2011.09.006>
- 646 Blacknell, C., 1981. Sandy gravel accumulation in a fluvial environment. *Geological Journal* 16,  
647 287–97. <https://doi.org/10.1002/gj.3350160407>

648 Blacknell, C., 1982. Morphology and surface sedimentary features of point bars in Welsh gravel-  
649 bed rivers. *Geological Magazine* 119, 181–192.

650 Bluck, B.J., 1979. Structure of coarse grained braided stream alluvium. *Transactions of the Royal*  
651 *Society of Edinburgh* 70, 181–221.

652 Blum, M.D., Törnqvist, T.E., 2000. Fluvial responses to climate and sea-level change: a review  
653 and look forward. *Sedimentology* 47, 2–48. <https://doi.org/10.1046/j.1365-3091>

654 Bond, G., Showers, W., Cheseby, M., Lotti, R., Almasi, P., DeMenocal, P., Priore, P., Cullen, H.,  
655 Hajdas, I., Bonani, G., 1997. A pervasive millennial-scale cycle in North Atlantic Holocene  
656 and glacial climates. *Science* 278(5341), 1257–1266.  
657 <https://doi.org/10.1126/science.278.5341.1257>

658 Bøtter-Jensen, L., 1997. Luminescence techniques: instrumentation and methods. *Radiation*  
659 *Measurements* 27(5–6), 749–768. [https://doi.org/10.1016/S1350-4487\(97\)00206-0](https://doi.org/10.1016/S1350-4487(97)00206-0)

660 Bøtter-Jensen, L., Bulur, E., Duller, G.A.T., Murray, A.S., 2000. Advances in luminescence  
661 instrument systems. *Radiation Measurements* 32(5–6), 523–528.  
662 [https://doi.org/10.1016/S1350-4487\(00\)00039-1](https://doi.org/10.1016/S1350-4487(00)00039-1)

663 Bradley S, Milne G, Shennan I, Edwards, R., 2011. An improved Glacial Isostatic Adjustment  
664 model for the British Isles. *Journal of Quaternary Science* 26, 541–552.  
665 <https://doi.org/10.1002>

666 Bradley, S.L., Ely, J.C., Clark, C.D., Edwards, R.J., Shennan, I., 2023. Reconstruction of the  
667 palaeo-sea level of Britain and Ireland arising from empirical constraints of ice extent:  
668 implications for regional sea level forecasts and North American ice sheet volume. *Journal*  
669 *of Quaternary Science*, 1-15. <https://doi:10.1002/jqs.3523>

670 Brennan, B.J., Lyons, R.G., Phillips, S.W., 1991 Attenuation of alpha particle track dose for  
671 spherical grains. *International Journal of Radiation Applications and Instrumentation. Part*  
672 *D. Nuclear Tracks and Radiation Measurements* 18, 249-253.

673 Bridge, J. S., 2009. Rivers and floodplains: forms, processes, and sedimentary record. Wiley.

674 Bridgland, D.R., (Ed.), 1986. Clast Lithological Analysis, QRA Technical Guide 3. Quaternary  
675 Research Association, London, p. 207.

676 Bridgland, D.R., Westaway, R., Howard, A.J. Innes, J.B., Long, A.J., Mitchell, W.A., White, M.J.,  
677 White, T.S., 2010. The role of glacio-isostasy in the formation of post-glacial river terraces  
678 in relation to the MIS 2 ice limit: evidence from northern England. *Proceedings of the*  
679 *Geologists' Association* 121, 113–127. <https://doi.org/10.1016/j.pgeola.2009.11.004>

680 Brierley, G.J., Hickin, E.J., 1991. Channel planform as a non-controlling factor in fluvial  
681 sedimentology: the case of the Squamish River floodplain, British Columbia. *Sedimentary*  
682 *Geology* 75(1–2), 67–83. [https://doi.org/10.1016/0037-0738\(91\)90051-E](https://doi.org/10.1016/0037-0738(91)90051-E)

683 Bronk Ramsey, C., 2008. Deposition models for chronological records. *Quaternary Science*  
684 *Reviews* 27(1-2), 42-60. <https://doi.org/10.1016/j.quascirev.2007.01.019>

685 Bronk Ramsey, C., 2009. Bayesian analysis of radiocarbon dates. *Radiocarbon* 51(1), 337-360.  
686 <https://doi.org/10.1017/S0033822200033865>

687 Bronk Ramsey, C., 2021. OxCal v4. 4.4. Available at: Retrieved from  
688 <https://c14.arch.ox.ac.uk/oxcal.html>

689 Brown, A.G., Toms, P.S., Carey, C.J., Howard, A.J.,  
690 Challis, K., 2013. Late Pleistocene–Holocene river dynamics at the Trent-Soar confluence,  
691 England, UK. *Earth Surface Processes and Landforms* 38(3), 237-  
692 249. <https://doi.org/10.1002/esp.3270>

693 Brunsdon, D., Thornes, J.B., 1979. Landscape sensitivity and change. *Transactions of the*  
694 *Institute of British Geographers* 4, 463–484. <https://doi.org/10.2307/622210>

695 Buck, C.E., Cavanagh, W.G., Litton, C.D., 1996. Bayesian approach to interpreting archaeological  
696 data. Wiley, Chichester, p. 404.

697 Charman, D.J., Blundell, A., Chiverrell, R.C., Hendon, D., Langdon, P.G., 2006. Compilation of  
698 non-annually resolved Holocene proxy climate records: stacked Holocene peatland  
699 palaeo-water table reconstructions from northern Britain. *Quaternary Science Reviews* 25,  
700 336–350. <https://doi.org/10.1016/j.quascirev.2005.05.005>

701 Chiverrell, R.C., Foster, G.C., Marshall, P., Harvey, A.M., Thomas, G.S.P., 2009a. Coupling  
702 relationships: Hillslope-fluvial linkages in the Hodder catchment, NW England.  
703 *Geomorphology* 109, 222–235. <https://doi.org/10.1016/j.geomorph.2009.03.004>

704 Chiverrell, R.D.C., Foster, G.C., Thomas, G.S.P., Marshall, P., Hamilton, D., 2009b. Robust

704 chronologies for landform development. *Earth Surface Processes and Landforms* 34(2),  
705 319-328. <https://doi.org/10.4002/esp.1720>

706 Chiverrell, R.C., Foster, G.C., Thomas, G.S.P., Marshall, P., 2010. Sediment transmission and  
707 storage: the implications for reconstructing landform development. *Earth Surface*  
708 *Processes and Landforms* 35, 4–15. <https://doi.org/10.1002/esp.1806>

709 Clark, C.D., Ely, J.C., Hindmarsh, R.C., Bradley, S., Ignéczi, A., Fabel, D., Ó Cofaigh, C.,  
710 Chiverrell, R.C., Scourse, J., Benetti, S., Bradwell, T., Evans, D.J.A., Roberts, D.H.,  
711 Burke, M., Callard, S. L., Medialdea, A., Saher, M., Small, D., Smedley, R.K., Gasson, E.,  
712 Gregoire, L., Gandy, N., Hughes, A.L.C., Ballantyne, C., Bateman, M.D., Bigg,  
713 G.R., Doole, J., Dayton, D., Duller, G.A.T., Jenkins, G.T.H., Livingstone, S.L., McCarron,  
714 S., Moreton, S., Pollard, D., Praeg, D., Sejrup, HP., Van Landeghem, K.J.J., Wilson, P.,  
715 2022. Growth and retreat of the last British–Irish Ice Sheet, 31 000 to 15 000 years ago:  
716 the BRITICE-CHRONO reconstruction. *Boreas* 51(4), 699-758.  
717 <https://doi.org/10.1111/bor.12594>

718 Collins, P.E., Worsley, P., Keith-Lucas, D.M., Fenwick, I.M., 2006. Floodplain environmental  
719 change during the Younger Dryas and Holocene in Northwest Europe: Insights from the  
720 lower Kennet Valley, south central England. *Palaeogeography, Palaeoclimatology,*  
721 *Palaeoecology* 233(1-2), 113-133. <https://doi.org/10.1016/j.palaeo.2005.09.01>

722 Cumming, J.S., 1971. Rockhead relief of southeast Northumberland and the lower Tyne Valley.  
723 Department of Geography Seminar Papers No. 18. University of Newcastle upon Tyne.

724 Cumming, J.S., 1977. A descriptive account of the buried rockhead topography of Tyneside. In:  
725 Fullerton, B. (Ed.), *North Eastern Studies*. Department of Geography, Newcastle upon  
726 Tyne, pp. 57–65.

727 Davies, B.J., Roberts, D.H., Ó Cofaigh, C., Bridgland, D.R., Riding, J., Phillips, E., Teasdale, D.,  
728 2009. Interlobate ice-sheet dynamics during the Last Glacial Maximum at Whitburn Bay,  
729 County Durham, England. *Boreas* 38, 555–578. [https://doi.org/10.1111/j.1502-](https://doi.org/10.1111/j.1502-3885.2008.00083.x)  
730 [3885.2008.00083.x](https://doi.org/10.1111/j.1502-3885.2008.00083.x)

- 731 Desloges, J.R., Church, M., 1987. Channel and floodplain facies in a wandering gravel-bed river.  
732 In: Ethridge, F.G., Flores, R.M., Harvey, M.D. (Eds.), Recent Developments in Fluvial  
733 Sedimentology. Society of Economic Paleontologists and Mineralogists, Special  
734 Publication 39, Oklahoma, USA, pp. 99–109.
- 735 Durcan, J.A., King, G.E., Duller, G.A.T., 2015 DRAC: Dose rate and age calculator for trapped  
736 charge dating. *Quaternary Geochronology* 28, 54-61.  
737 <https://doi.org/10.1016/j.quageo.2015.03.012>
- 738 Evans, I.S., 1999. Castle Eden Dene and Blunts Dene. In: Bridgland, D.R., Horton, B.P., Innes,  
739 J.B. (Eds.), The Quaternary of North-East England, QRA Field Guide, Quaternary  
740 Research Association, London, pp. 57–63.
- 741 Evans, D.J., Roberts, D.H., Bateman, M.D., Clark, C.D., Medialdea, A., Callard, L., Grimoldi, E.,  
742 Chiverrell, R.C., Ely, J., Dove, D., Ó Cofaigh, C., 2021. Retreat dynamics of the eastern  
743 sector of the British–Irish Ice Sheet during the last glaciation. *Journal of Quaternary*  
744 *Science* 36(5), 723-751. <https://doi:10.1002/jqs.3275>
- 745 Ferguson, R.I., Werritty, A., 1983. Bar development and channel changes in the gravelly River  
746 Feshie, Scotland. In: Collinson, J.D., Lewin, J. (Eds.), Modern and Ancient Fluvial  
747 Systems, Special Publication of the International Association of Sedimentologists 6.  
748 Blackwell, Oxford, pp. 181–193. <https://doi.org/10.1002/9781444303773.ch14>
- 749 Forbes, D.L., 1983. Morphology and sedimentology of a sinuous gravel-bed channel system:  
750 lower Babbage River, Yukon coastal plain, Canada. In: Collinson, J.D., Lewin, J. (Eds.),  
751 Modern and Ancient Fluvial Systems, Special Publication of the International Association  
752 of Sedimentologists 6. Blackwell, Oxford, pp. 195–206.  
753 <https://doi.org/10.1002/9781444303773.ch15>
- 754 Foster, G.C., Chiverrell, R.C., Thomas, G.S.P., Marshall, P., Hamilton, D., 2009. Fluvial  
755 development and the sediment regime of the lower Calder, Ribble catchment, northwest  
756 England. *Catena* 77, 81–95. <https://doi.org/10.1016/j.catena.2008.09.006>
- 757 Fryirs, K.A., 2017. River sensitivity: a lost foundation concept in fluvial geomorphology. *Earth*  
758 *Surface Processes and Landforms* 42(1), 55–70. <https://doi.org/10.1002/esp.3940>

- 759 Galbraith, R.F., Laslett, G.M., 1993. Statistical models for mixed fission track ages. *Nuclear tracks*  
760 *and radiation measurements* 21(4), 459–470. [https://doi.org/10.1016/1359-](https://doi.org/10.1016/1359-0189(93)90185-C)  
761 [0189\(93\)90185-C](https://doi.org/10.1016/1359-0189(93)90185-C)
- 762 Galbraith, R.F., Roberts, R.G., Laslett, G.M., Yoshida, H., Olley, J.M., 1999. Optical dating of  
763 single and multiple grains of quartz from Jinmium rock shelter, northern Australia: Part I,  
764 experimental design and statistical models. *Archaeometry* 41(2), 339–364.  
765 <https://doi.org/10.1111/j.1475-4754.1999.tb00988.x>
- 766 Gao, C., Boreham, S., Preece, R.C., Gibbard, P.L., Briant, R.M., 2007. Fluvial response to rapid  
767 climate change during the Devensian (Weichselian) Lateglacial in the River Great Ouse,  
768 southern England, UK. *Sedimentary Geology* 202(1-2), 193-210.  
769 <https://doi.org/10.1016/j.sedgeo.2007.02.004>
- 770 Ghilardi, B., O'Connell, M., 2013. Early Holocene vegetation and climate dynamics with particular  
771 reference to the 8.2 ka event: pollen and macrofossil evidence from a small lake in  
772 western Ireland. *Vegetation history and archaeobotany* 22, 99–114.  
773 <https://doi.org/10.1007/s00334-012-0367-x>
- 774 Gibbard, P.L., Lewin, J., 2002. Climate and related controls on interglacial fluvial sedimentation in  
775 lowland Britain. *Sedimentary Geology* 151(3–4), 187–210. [https://doi.org/10.1016/S0037-](https://doi.org/10.1016/S0037-0738(01)00253-6)  
776 [0738\(01\)00253-6](https://doi.org/10.1016/S0037-0738(01)00253-6)
- 777 Golledge, N.R., 2010. Glaciation of Scotland during the Younger Dryas stadial: a review. *Journal*  
778 *of Quaternary Science* 25, 550–566. <https://doi.org/10.1002/jqs.1319>
- 779 Guérin, G., Mercier, N., Adamiec, G., 2011. Dose-rate conversion factors: update. *Ancient*  
780 *TL* 29(1), 5–8.
- 781 Guérin, G., Mercier, N., Nathan, R., Adamiec, G., Lefrais, Y., 2012. On the use of the infinite  
782 matrix assumption and associated concepts: A critical review. *Radiation Measurements*  
783 47, 778-785. <https://doi.org/10.1016/j.radmeas.2012.04.004>
- 784 Harrison, S., Bailey, R.M., Anderson, E., Arnold, L., Douglas, T., 2010. Optical Dates from British  
785 Isles 'Solifluction Sheets' Suggests Rapid Landscape Response to Late Pleistocene

786 Climate Change. *Scottish Geographical Journal* 126, 101–111.  
787 <https://doi.org/10.1080/14702541003712911>

788 Harrison, S., Hughes, L., Glasser, N., Kuras, O., 2021. Late Quaternary solifluction sheets in the  
789 British uplands. *Journal of Quaternary Science* 36(7), 1162–1173.  
790 <https://doi.org/10.1002/jqs.3369>

791 Harvey, A.M., Renwick, W.H., 1987. Holocene alluvial fan and terrace formation in the Bowland  
792 Fells Northwest England. *Earth Surface Processes and Landforms* 12, 249–  
793 257. <https://doi.org/10.1002/esp.3290120304>

794 Hill, T.C., Woodland, W.A., Spencer, C.D., Marriott, S.B., Case, D.J. and Catt, J.A., 2008.  
795 Devensian late-glacial environmental change in the Gordano Valley, North Somerset,  
796 England: a rare archive for southwest Britain. *Journal of paleolimnology* 40, 431-444.

797 Hooke, J., 2003. River meander behaviour and instability: a framework for analysis. *Transactions*  
798 *of the Institute of British Geographers* 28, 238–253. [https://doi.org/10.1111/1475-](https://doi.org/10.1111/1475-5661.00089)  
799 [5661.00089](https://doi.org/10.1111/1475-5661.00089)

800 Hooke, J. M., 2004. Cutoffs galore!: occurrence and causes of multiple cutoffs on a meandering  
801 river. *Geomorphology* 61, 225–238. <https://doi.org/10.1016/j.geomorph.2003.12.006>

802 Horton, B.P., Innes, J.B., Shennan, I., 1999a. Late Devensian and Holocene relative sea-level  
803 changes in Northumberland, England. In: Bridgland, D.R., Horton, B.P., Innes, J.B. (Eds.),  
804 The Quaternary of North-East England, QRA Field Guide. Quaternary Research  
805 Association, London, pp. 35–47.

806 Horton, B.P., Innes, J.B., Plater, A.J., Tooley, M.J., Wright, M.R., 1999b. Post-glacial evolution  
807 and relative sea-level changes in Hartlepool Bay and the Tees estuary. In: Bridgland,  
808 D.R., Horton, B.P., Innes, J.B. (Eds.), The Quaternary of North-East England, QRA Field  
809 Guide. Quaternary Research Association, London, pp. 65–86.

810 Howard, A.J., Carney, J.N., Greenwood, M.T., Keen, D.H., Mighall, T., O'Brien, C. and Tetlow, E.,  
811 2011. The Holme Pierrepont sand and gravel and the timing of Middle and Late  
812 Devensian floodplain aggradation in the English Midlands. *Proceedings of the Geologists'*  
813 *Association* 122(3), 419-431.

814 Howard, A.J., Macklin, M.G., Black, S., Hudson-Edwards, K.A., 2000a. Holocene river  
815 development and environmental change in Upper Wharfedale, Yorkshire Dales,  
816 England. *Journal of Quaternary Science* 15(3), 239–252.  
817 [https://doi.org/10.1002/\(SICI\)1099-1417\(200003\)15:3<239::AID-JQS480>3.0.CO;2-W](https://doi.org/10.1002/(SICI)1099-1417(200003)15:3<239::AID-JQS480>3.0.CO;2-W)

818 Howard, A.J., Keen, D.H., Mighall, T.M., Field, M.H., Coope, G.R., Griffiths, H.I., Macklin, M.G.,  
819 2000b. Early Holocene environments of the River Ure near Ripon, North Yorkshire,  
820 UK. *Proceedings of the Yorkshire Geological Society* 53(1), 31–41.

821 Hughes, A. L., Clark, C. D., Jordan, C. J. 2014. Flow-pattern evolution of the last British Ice  
822 Sheet. *Quaternary Science Reviews* 89, 148–168.  
823 <https://doi.org/10.1016/j.quascirev.2014.02.002>

824 Hughes, P.D., Clark, C.D., Gibbard, P.L., Glasser, N.F., Tomkins, M.D., 2023. Britain and Ireland:  
825 glacial landforms during deglaciation. In: Palacios, D., Hughes, P.D., García-Ruiz, J.,  
826 Andrés, N. (Eds.), *European Glacial Landscapes, The Last Deglaciation*. Elsevier,  
827 London, pp. 129–139. <https://doi.org/10.1016/B978-0-323-91899-2.00027-9>

828 Hughes, P.D.M., Mauquoy, D., Barber, K.E., Langdon, P.G., 2000. Mire-development pathways  
829 and palaeoclimatic records from a full Holocene peat archive at Walton Moss, Cumbria,  
830 England. *The Holocene* 10, 465–479. <https://doi.org/10.1016/j.quascirev.2014.02.002>

831 Innes, J.B., 1999. Regional Vegetational History. In: Bridgland, D.R., Horton, B.P., Innes, J.B.  
832 (Eds.), *The Quaternary of North-East England, QRA Field Guide*. Quaternary Research  
833 Association, Cambridge, pp. 21–34.

834 Innes, J., Mitchell, W., O'brien, C., Roberts, D., Rutherford, M., Bridgland, D., 2021. A Detailed  
835 Record of Deglacial and Early Post-Glacial Fluvial Evolution: The River Ure in North  
836 Yorkshire, UK. *Quaternary* 4(1), p. 9. <https://doi.org/10.3390/quat4010009>

837 Johnson, G.A.L., 1997. Geology of Hadrian's Wall. *Geologists' Association Guide* 59. Geologists'  
838 Association, London, p. 89.

839 Jones, A.P., Tucker, M.E., Hart, J.K., 1999. The Description and Analysis of Quaternary  
840 Stratigraphic Field Sections. *QRA Technical Guide* 7. Quaternary Research Association,  
841 London. p. 286.



- 842 Kreutzer, S., Schmidt, C., Fuchs, M.C., Dietze, M., Fischer, M. and Fuchs, M. 2012 Introducing an  
843 R package for luminescence dating analysis. *Ancient TL* 30, pp. 1-8
- 844 Lang, B., Bedford, A., Brooks, S.J., Jones, R.T., Richardson, N., Birks, H. J.B., Marshall, J.D.  
845 2010. Early-Holocene temperature variability inferred from chironomid assemblages at  
846 Hawes Water, northwest England. *The Holocene* 20, 943–954.  
847 <https://doi.org/10.1177/0959683610366157>
- 848 Lewin, J., Gibbard, P.L., 2010. Quaternary river terraces in England: forms, sediments and  
849 processes. *Geomorphology*, 120(3-4), 293-311.  
850 <https://doi.org/10.1016/j.geomorph.2010.04.002>
- 851 Lewin, J., Macklin, M.G., 2003. Preservation potential for Late Quaternary river alluvium. *Journal*  
852 *of Quaternary Science* 18, 107–120. <https://doi.org/10.1002/jqs.738>
- 853 Lewin, J., Macklin, M.G., Johnstone, E., 2005. Interpreting alluvial archives: sedimentological  
854 factors in the British Holocene fluvial record. *Quaternary Science Reviews* 24, 1873–1889.  
855 <https://doi.org/10.1016/j.quascirev.2005.01.009>
- 856 Livingstone, S.J., Evans, D.J., Cofaigh, C.Ó., Davies, B.J., Merritt, J.W., Huddart, D., Mitchell,  
857 W.A., Roberts, D.H., Yorke, L. 2012. Glaciodynamics of the central sector of the last  
858 British–Irish Ice Sheet in Northern England. *Earth-Science Reviews* 111, 25–55.  
859 <https://doi.org/10.1016/j.earscirev.2011.12.006>
- 860 Livingstone, S.J., Roberts, D.H., Davies, B.J., Evans, D.J., Ó Cofaigh, C., Gheorghiu, D.M., 2015.  
861 Late Devensian deglaciation of the Tyne Gap Palaeo-Ice stream, northern  
862 England. *Journal of Quaternary Science* 30(8), 790–804. <https://doi.org/10.1002/jqs.2813>
- 863 Lowe, J.J., Rasmussen, S.O., Björck, S., Hoek, W.Z., Steffensen, J.P., Walker, M.J.C., Yu, Z.C.,  
864 2008. Synchronisation of palaeoenvironmental events in the North Atlantic region during  
865 the last termination: a revised protocol recommended by the INTIMATE group.  
866 *Quaternary Science Reviews* 27, 6–17. <https://doi.org/10.1016/j.quascirev.2007.09.016>
- 867 Macklin, M.G., 1999. Holocene river environments in prehistoric Britain: human interaction and  
868 impact. *Journal of Quaternary Science* 14, 521–530. [https://doi.org/10.1002/\(SICI\)1099-1417\(199910\)14:6<521::AID-JQS487>3.0.CO;2-G](https://doi.org/10.1002/(SICI)1099-1417(199910)14:6<521::AID-JQS487>3.0.CO;2-G)  
869

- 870 Macklin, M.G., Lewin, J., 1993. Holocene river alluviation in Britain. *Zeitschrift für*  
871 *Geomorphologie* 47, 109–122.
- 872 Macklin, M.G., Lewin, J., Jones, A.F., 2013. River entrenchment and terrace formation in the UK  
873 Holocene. *Quaternary Science Reviews* 76, 194–206.  
874 <https://doi.org/10.1016/j.quascirev.2013.05.026>
- 875 Macklin, M.G., Lewin, J., Jones, A.F., 2014. Anthropogenic alluvium: An evidence-based meta-  
876 analysis for the UK Holocene, *Anthropocene* 6, 26–38.  
877 <https://doi.org/10.1016/j.ancene.2014.03.003>
- 878 Macklin, M.G., Rumsby, B.T., 2007. Changing climate and extreme floods in the British  
879 uplands. *Transactions of the Institute of British Geographers* 32(2), 68–186.  
880 <https://doi.org/10.1111/j.1475-5661.2007.00248.x>
- 881 Macklin, M.G., Rumsby, B.T., Heap, T., 1992. Flood alluviation and entrenchment: Holocene  
882 valley-floor development and transformation in the British uplands. *Geological Society of*  
883 *America Bulletin* 104(6), 631–643. [https://doi.org/10.1130/0016-](https://doi.org/10.1130/0016-7606(1992)104<0631:FAAEHV>2.3.CO;2)  
884 [7606\(1992\)104<0631:FAAEHV>2.3.CO;2](https://doi.org/10.1130/0016-7606(1992)104<0631:FAAEHV>2.3.CO;2)
- 885 Mahan, S.A., Rittenour, T.M., Nelson, M.S., Atae, N., Brown, N., DeWitt, R., Durcan, J., Evans,  
886 M., Feathers, J., Frouin, M. and Guérin, G., 2023. Guide for interpreting and reporting  
887 luminescence dating results. *GSA Bulletin* 135(5-6), 1480-1502.  
888 <https://doi.org/10.1130/B36404.1>
- 889 Mayewski, P.A., Rohling, E.E., Stager, J.C., Karlen, W., Maasch, K.A., Meeker, L.D., Meyerson,  
890 E.A., Gasse, F., van Kreveld, S., Holmgren, K., Lee-Thorp, J., Rosqvist, G., Rack, F.,  
891 Staubwasser, M., Schneider, R.R., Steig, E.J., 2004. Holocene climate variability.  
892 *Quaternary Research* 62, 243–255. <https://doi.org/10.1016/j.yqres.2004.07.001>
- 893 Mejdahl, V., 1979. Thermoluminescence dating: beta-dose attenuation in quartz  
894 grains. *Archaeometry* 21(1), 61–72.
- 895 Miall, A.D., 1988. Facies architecture in clastic sedimentary basins. In: Kleinspehn, K.L., Paolo, C.  
896 (Eds.) *New perspectives in basin analysis*. *Frontiers in Sedimentary Geology*. Springer,  
897 New York, pp. 67–81.

- 898 Miall, A.D. 1996. The Geology of Fluvial Deposits: Sedimentary Facies, Basin Analysis and  
899 Petroleum Geology. Springer-Verlag, Berlin, p. 582. [https://doi.org/10.1007/987-3-662-](https://doi.org/10.1007/987-3-662-03237-4)  
900 [03237-4](https://doi.org/10.1007/987-3-662-03237-4)
- 901 Mills, D.A.C., Holliday, D.W., 1998. Geology of the district around Newcastle upon Tyne,  
902 Gateshead and Consett: Memoir for the 1: 50,000 Geological Sheet 20. HMSO, London,  
903 p. 162.
- 904 Mol, J., Vandenberghe, J., Kasse, C., 2000. River response to variations of periglacial climate in  
905 mid-latitude Europe. *Geomorphology* 33(3–4), 131–148. [https://doi.org/10.1016/S0169-](https://doi.org/10.1016/S0169-555X(99)00126-9)  
906 [555X\(99\)00126-9](https://doi.org/10.1016/S0169-555X(99)00126-9)
- 907 Moores, A.J., 1998. Palaeoenvironmental investigations of Holocene landscapes in the North  
908 Tyne basin, northern England. Unpublished PhD thesis, Newcastle University.  
909 <http://theses.ncl.ac.uk/jspui/handle/10443/2211>
- 910 Moores, A.J., Passmore, D.G., Stevenson, A.C., 1999. High resolution palaeochannel records of  
911 Holocene valley floor environments in the North Tyne basin, northern England. In: Brown,  
912 A.G., Brown, A., Quine, T. (Eds.). *Fluvial processes and environmental change* (Vol. 13).  
913 Wiley-Blackwell, Chichester, pp. 283–310.
- 914 Murray, A.S., Olley, J.M., Caitcheon, G.G. 1995. Measurement of equivalent doses in quartz from  
915 contemporary water-lain sediments using optically stimulated luminescence. *Quaternary*  
916 *Science Reviews* 14, 365–371.
- 917 Murray, A.S, Wintle, A.G., 2000. Luminescence dating of quartz using an improved single-aliquot  
918 regenerative-dose protocol. *Radiation measurements* 32(1), 57–73.  
919 [https://doi.org/10.1016/S1350-4487\(99\)00253-X](https://doi.org/10.1016/S1350-4487(99)00253-X)
- 920 Nesje, A., Lie, Ø., Dahl, S.O., 2000. Is the North Atlantic Oscillation reflected in Scandinavian  
921 glacier mass balance records? *Journal of Quaternary Science* 15(6), 587–601.  
922 [https://doi.org/10.1016/S0277-3791\(99\)00090-6](https://doi.org/10.1016/S0277-3791(99)00090-6)
- 923 Notebaert, B., Verstraeten, G., 2010. Sensitivity of West and Central European river systems to  
924 environmental changes during the Holocene: A review. *Earth-Science Reviews* 103(3–4),  
925 163–182. <https://doi.org/10.1016/j.earscirev.2010.09.009>

926 Passmore, D.G., Macklin, M.G., 1994. Provenance of fine-grained alluvium and late Holocene  
927 land-use change in the Tyne basin, northern England. *Geomorphology* 9(2), 127–142.  
928 [https://doi.org/10.1016/0169-555X\(94\)90071-X](https://doi.org/10.1016/0169-555X(94)90071-X)

929 Passmore, D.G., Macklin, M.G., 2000. Late Holocene channel and floodplain development in a  
930 wandering gravel-bed river: the River South Tyne at Lambley, Northern England. *Earth*  
931 *Surface Processes and Landforms* 25, 1237–1256. [https://doi.org/10.1002/1096-  
932 9837\(200010\)25:11<1237::AID-ESP134>3.0.CO;2-S](https://doi.org/10.1002/1096-9837(200010)25:11<1237::AID-ESP134>3.0.CO;2-S)

933 Passmore, D.G., Waddington, C., 2009. Paraglacial adjustment of the fluvial system to Late  
934 Pleistocene deglaciation: the Milfield Basin, northern England. Geological Society,  
935 London. Special Publications 320(1),145–164. <https://doi.org/10.1144/SP320.10>

936 Peel, R.F., 1941. The North Tyne Valley. *The Geographical Journal* 98, 5–19.

937 Philips, J.D., 2010. Amplifiers, filters and geomorphic responses to climate change in Kentucky  
938 rivers. *Climate Change* 103, 571–595. <https://doi.org/10.1007/s10584-009-9775-z>

939 Pope, A., 2017. SRTM shaded relief DEM of Great Britain, [Dataset]. University of Edinburgh.  
940 <https://doi.org/10.7488/ds/1722>

941 Rasmussen, S.O., Bigler, M., Blockley, S.P., Blunier, T., Buchardt, S.L., Clausen, H.B.,  
942 Cvijanovic, I., Dahl-Jensen, D., Johnsen, J.L., Fischer, H., Gkinis, V., Guillevic, M., Hoek,  
943 W.Z., Lowe, J.J., Pedro, J.B., Popp, T., Seierstad, I.K., Steffensen, J.P., Svensson, A.M.,  
944 Vallengø, P., Vinther, B.M., Walker, M.J.C., Wheatley, J.J., Winstrup, M., 2014. A  
945 stratigraphic framework for abrupt climatic changes during the Last Glacial period based  
946 on three synchronized Greenland ice-core records: refining and extending the INTIMATE  
947 event stratigraphy. *Quaternary Science Reviews* 106, 14–28.  
948 <https://doi.org/10.1016/j.quascirev.2014.09.007>

949 Reimer, P.J., Austin, W.E., Bard, E., Bayliss, A., Blackwell, P.G., Ramsey, C.B., Butzin, M.,  
950 Cheng, H., Edwards, R.L., Friedrich, M., Grootes, P.M., 2020. The IntCal20 Northern  
951 Hemisphere radiocarbon age calibration curve (0–55 cal kBP). *Radiocarbon* 62(4),725-  
952 757. <https://doi:10.1017/RDC.2020.41>

953 Rice, S.P., Church, M., Wooldridge, C.L., Hickin, E.J., 2009. Morphology and evolution of bars in  
954 a wandering gravel-bed river; lower Fraser river, British Columbia, Canada.  
955 *Sedimentology* 56, 709–736. <https://doi.org/10.1111/j.1365-3091.2008.00994.x>

956 Rice, S. P., Church, M., 2010. Grain-size sorting within river bars in relation to downstream fining  
957 along a wandering channel. *Sedimentology* 57, 232–251. [https://doi.org/10.1111/j.1365-](https://doi.org/10.1111/j.1365-3091.2009.01108.x)  
958 [3091.2009.01108.x](https://doi.org/10.1111/j.1365-3091.2009.01108.x)

959 Roberts, D.H., Evans, D.J., Callard, S.L., Clark, C.D., Bateman, M.D., Medialdea, A., Dove, D.,  
960 Cotterill, C.J., Saher, M., Cofaigh, C.Ó., Chiverrell, R.C., 2018. Ice marginal dynamics of  
961 the last British-Irish Ice Sheet in the southern North Sea: Ice limits, timing and the  
962 influence of the Dogger Bank. *Quaternary Science Reviews* 198, 181–207.  
963 <https://doi.org/10.1016/j.quascirev.2018.08.010>

964 Rumsby, B. T., Macklin, M. G., 1996. River response to the last neoglacial (the ‘Little Ice Age’) in  
965 northern, western and central Europe. Geological Society, London, Special Publications  
966 115, 217–233.

967 Scrutton, C.T., 1995. Northumbria Rocks and Landscape. Ellenbank, Leeds, p. 216.

968 Shakun, J.D., Carlson, A.E. 2010. A global perspective on Last Glacial Maximum to Holocene  
969 climate change. *Quaternary Science Reviews* 29, 1801–1816.  
970 <https://doi.org/10.1016/j.quascirev.2010.03.016>

971 Shennan, I., Bradley, S.L., Edwards, R., 2018. Relative sea-level changes and crustal  
972 movements in Britain and Ireland since the Last Glacial Maximum. *Quaternary Science*  
973 *Reviews* 188, 143-159. <https://doi.org/10.1016/j.quascirev.2018.03.031>

974 Smith, D.B., 1994. Geology of the district around Sunderland. Memoir of the British Geological  
975 Survey Sheet 21. HMSO, London, p. 173.

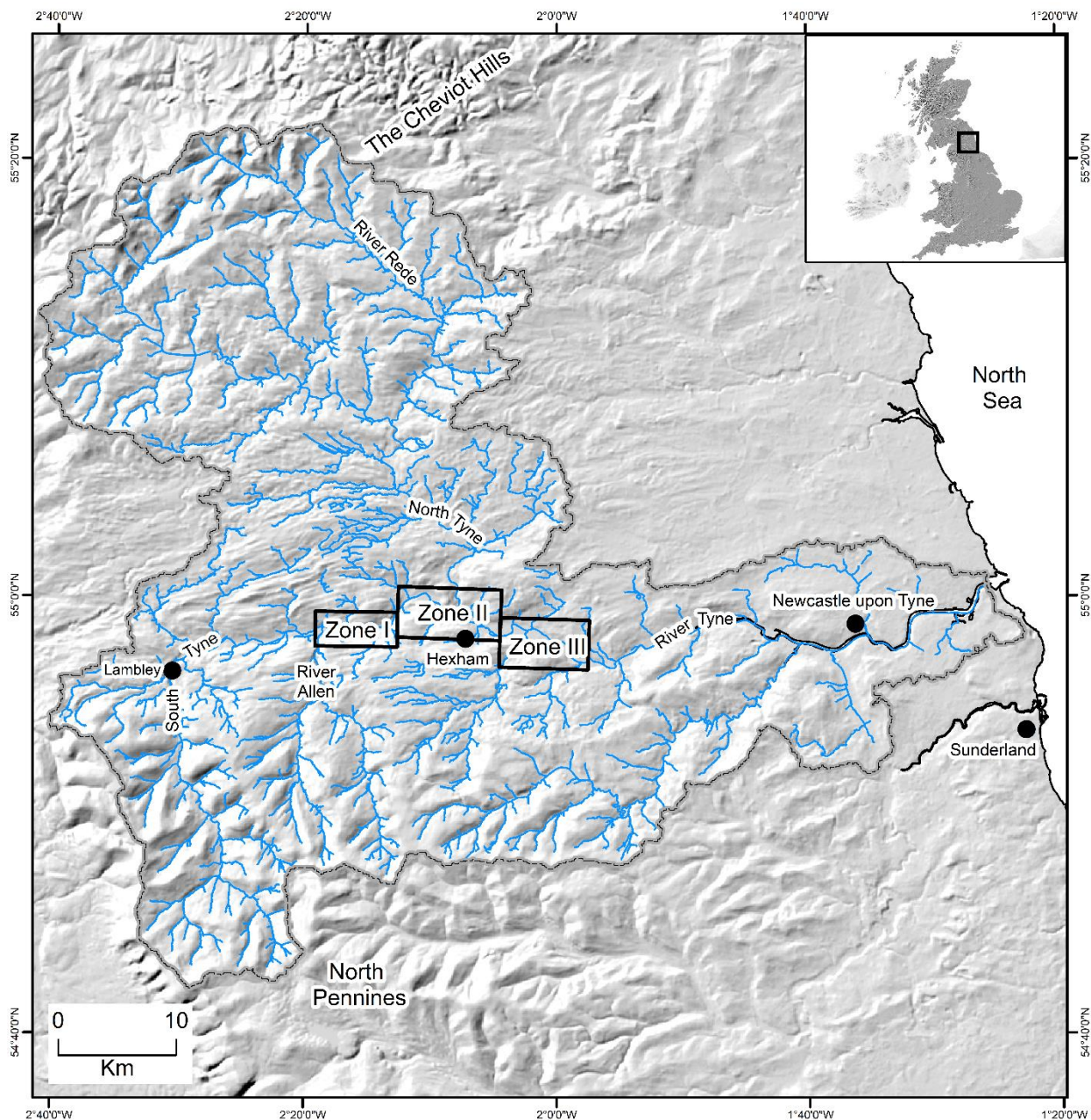
976 Smith, S.A., 1990. The sedimentology and accretionary styles of an ancient gravel bed stream:  
977 the Budleigh Salterton Pebble beds (Lower Triassic), southwest England. *Sedimentary*  
978 *Geology* 67, 199–219. [https://doi.org/10.1016/0037-0738\(90\)90035-R](https://doi.org/10.1016/0037-0738(90)90035-R)

- 979 Smith, G.H.S., Ashworth, P.J., Best, J.L., Lunt, I.A., Orfeo, O., Parsons, D.R., 2009. The  
980 sedimentology and alluvial architecture of a large braid bar, Río Paraná, Argentina.  
981 *Journal of Sedimentary Research* 79, 629–642. <https://doi.org/10.2110/jsr.2009.066>
- 982 Teasdale D. 2013. Evidence for the western limits of the North Sea Lobe of the BHS in North East  
983 England. In: QRA Field Guide: The Quaternary of Northumberland, Durham and  
984 Yorkshire, BJ Davies, B.J., Yorke, L., Bridgland, D.R., Roberts, D.H. (Eds). Quaternary  
985 Research Association, Cambridge, pp. 106–121.
- 986 Thornalley, D.J., Elderfield, H., McCave, I.N., 2009. Holocene oscillations in temperature and  
987 salinity of the surface subpolar North Atlantic. *Nature* 457, 711–714.  
988 <https://doi.org/10.1038/nature07717>
- 989 Thrasher, I., Mauz, B., Chiverrell, R.C., Lang, A., 2009. Luminescence dating of glaciofluvial  
990 deposits: A review. *Earth Science Reviews* 97, 133–146.  
991 <https://doi.org/10.1016/j.earscirev.2009.09.001>
- 992 Tipping, R., 1994. Fluvial chronology and valley floor evolution of the upper Bowmont valley,  
993 Borders Region, Scotland. *Earth surface processes and landforms* 19(7), 641-657.
- 994 Tipping, R., 1995. Holocene evolution of a lowland Scottish landscape: Kirkpatrick Fleming. Part I,  
995 peat-and pollen-stratigraphic evidence for raised moss development and climatic  
996 change. *The Holocene* 5(1), 69-81.
- 997 Tipping, R.M., Jones, A.P., Carter, S., Holden, T., Cressey, M., 2008. The chronology and long  
998 term dynamics of a low energy river system: the Kelvin Valley, central Scotland. *Earth*  
999 *Surface Processes and Landforms* 33, 910–922. <https://doi.org/10.1002/esp.158>
- 1000 Tipping, R.M., Milburn, P., Halliday, S., 1999. Fluvial processes, land use and climate change  
1001 2000 years ago in upper Annandale, southern Scotland. In: Brown, A.G., Quine, T.A.  
1002 (Eds). *Fluvial Processes and Environmental Change*. John Wiley & Sons, Chichester, pp.  
1003 311-327.
- 1004 Tolan-Smith, C., 1996. The Mesolithic/Neolithic transition in the North Tyne Valley: a landscape  
1005 approach. *Neolithic Studies in No-Man's Land: Papers on the Neolithic of Northern*  
1006 *England from the Trent to the Tweed*. *Northern Archaeology* 13(14), 7-16.

- 1007 Tucker, M.E., 2011. Sedimentary Rocks in the Field. The Geological Field Guide Series, 4<sup>th</sup> Ed.  
1008 Wiley, Chichester, p. 229.
- 1009 Vandenberghe, J., 2008. The fluvial cycle at cold–warm–cold transitions in lowland regions: a  
1010 refinement of theory. *Geomorphology* 98(3–4), 275–284.  
1011 <https://doi.org/10.1016/j.geomorph.2006.12.030>
- 1012 Vandenberghe, J., 2015. River terraces as a response to climatic forcing: formation processes,  
1013 sedimentary characteristics and sites for human occupation. *Quaternary International* 370,  
1014 3–11. <https://doi.org/10.1016/j.quaint.2014.05.046>
- 1015 van de Lageweg, W.I., van Dijk, W.M., Baar, A.W., Rutten, J., Kleinhans, M.G., 2014. Bank pull or  
1016 bar push: What drives scroll-bar formation in meandering rivers? *Geology* 42, 319–322.  
1017 <https://doi.org/10.1130/G35192.1>
- 1018 Vincent, P.J., Lord, T.C., Telfer, M.W., Wilson, P., 2011. Early Holocene loessic colluviation in  
1019 northwest England: new evidence for the 8.2 ka event in the terrestrial record? *Boreas* 40,  
1020 105–115. <https://doi.org/10.1111/j.1502-3885.2010.00172.x>
- 1021 Werritty, A., 2021. Fluvial Landforms of Glen Feshie and the Spey Drainage Basin. In: Ballantyne,  
1022 C.K., Gordon, J.E. (Eds) Landscapes and Landforms of Scotland. World  
1023 Geomorphological Landscapes. Springer, Cham. pp. 349–358.  
1024 [https://doi.org/10.1007/978-3-030-71246-4\\_19](https://doi.org/10.1007/978-3-030-71246-4_19)
- 1025 Whiting, P.J., Dietrich, W.E., Leopold, L.B., Drake, T.G., Shreve, R.L., 1988. Bedload sheets in  
1026 heterogeneous sediment. *Geology* 16, 105–108. [https://doi.org/10.1130/0091-7613\(1988\)016<0105:BSIHS>2.3.CO;2](https://doi.org/10.1130/0091-7613(1988)016<0105:BSIHS>2.3.CO;2)
- 1027
- 1028 Wilson, P., 2002. Morphology and significance of some Loch Lomond Stadial moraines in the  
1029 south-central Lake District, England. *Proceedings of the Geologists' Association* 113, 9–  
1030 21. [https://doi.org/10.1016/S0016-7878\(02\)80002-5](https://doi.org/10.1016/S0016-7878(02)80002-5)
- 1031 Wintle, A.G., 2008. Fifty years of luminescence dating. *Archaeometry* 50(2), pp.276-312.  
1032 <https://doi.org/10.1111/j.1475-4754.2008.00392.x>
- 1033 Wintle, A.G., Murray, A.S., 2006. A review of quartz optically stimulated luminescence  
1034 characteristics and their relevance in single-aliquot regeneration dating

- 1035 protocols. *Radiation measurements* 41(4), 369–391.
- 1036 <https://doi.org/10.1016/j.radmeas.2005.11.001>
- 1037 Wooldridge, C.L., Hickin, E.J., 2005. Radar architecture and evolution of channel bars in  
1038 wandering gravel-bed rivers: Fraser and Squamish rivers, British Columbia, Canada.  
1039 *Journal of Sedimentary Research* 75, 844–860. <https://doi.org/10.2110/jsr.2005.066>
- 1040 Yorke, L., 2008. Late Quaternary Valley Fill Sediments in the River Tyne Valley: Understanding  
1041 Late Devensian Deglaciation and Early Postglacial Response in Northern England.  
1042 Unpublished Ph.D. thesis, University of Hull. [https://hull-](https://hull-repository.worktribe.com/output/4209010)  
1043 [repository.worktribe.com/output/4209010](https://hull-repository.worktribe.com/output/4209010)
- 1044 Yorke, L., Rumsby, B.T., Chiverrell, R.C., 2012. Depositional history of the Tyne valley associated  
1045 with retreat and stagnation of Late Devensian Ice Streams. *Proceedings of the Geologists'*  
1046 *Association* 123, 608–625. <https://doi.org/10.1016/j.pgeola.2012.03.005>
- 1047 Zimmerman, J., 1971. The radiation-induced increase of the 100 C thermoluminescence  
1048 sensitivity of fired quartz. *Journal of Physics C: Solid State Physics* 4(18), 3265.



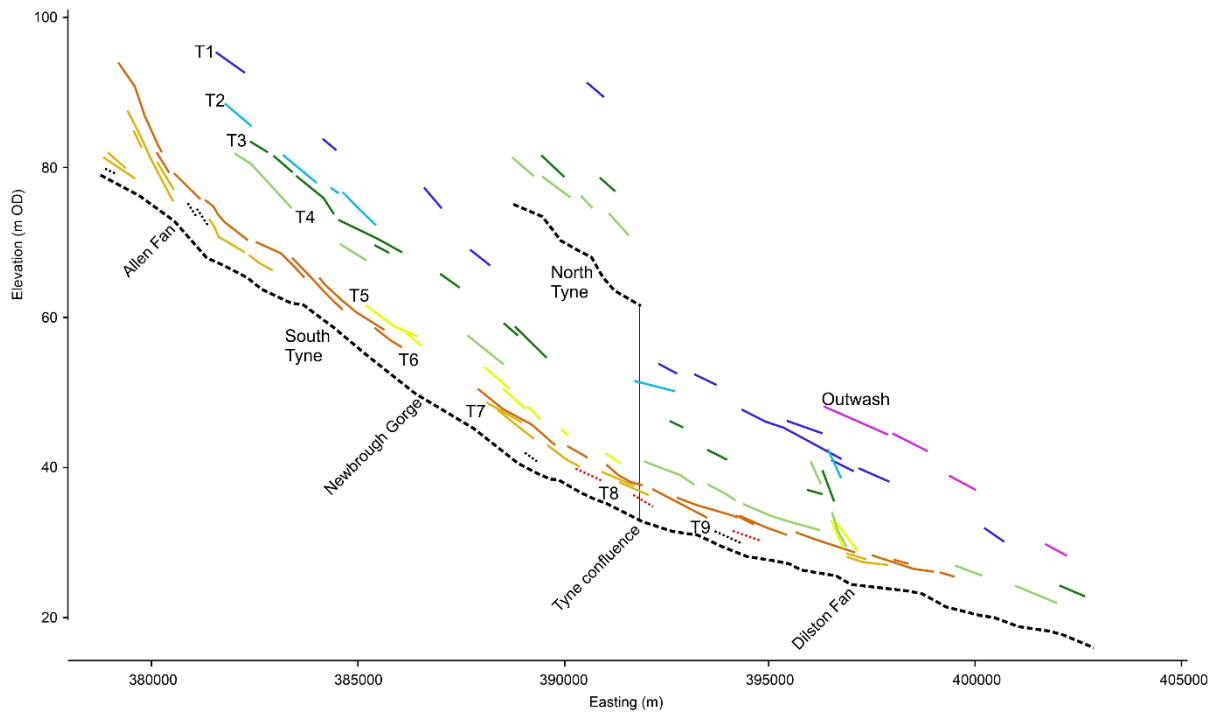


1049  
 1050 Figure 1. Extent of the Tyne catchment, with key rivers and places named. Overlain on a shaded  
 1051 relief SRTM DEM (Pope, 2017). The key locations in the mid-Tyne valley have been divided into  
 1052 three zones (I, II and III) and are demarcated by the black rectangles.

1053

1054

1055 Figure 2. Geomorphic map of the mid-Tyne valley, showing river terraces, palaeochannels  
 1056 (demarcated by double hashed lines) and alluvial fans, overlain on 1 m resolution LiDAR data and  
 1057 displayed as hillshade layers (© Environment Agency copyright (2023). All rights reserved). Key  
 1058 sites and localities are shown; (A) zone I, (B) zone II, and (C) zone III.



1059

1060

1061

1062

1063

1064

1065

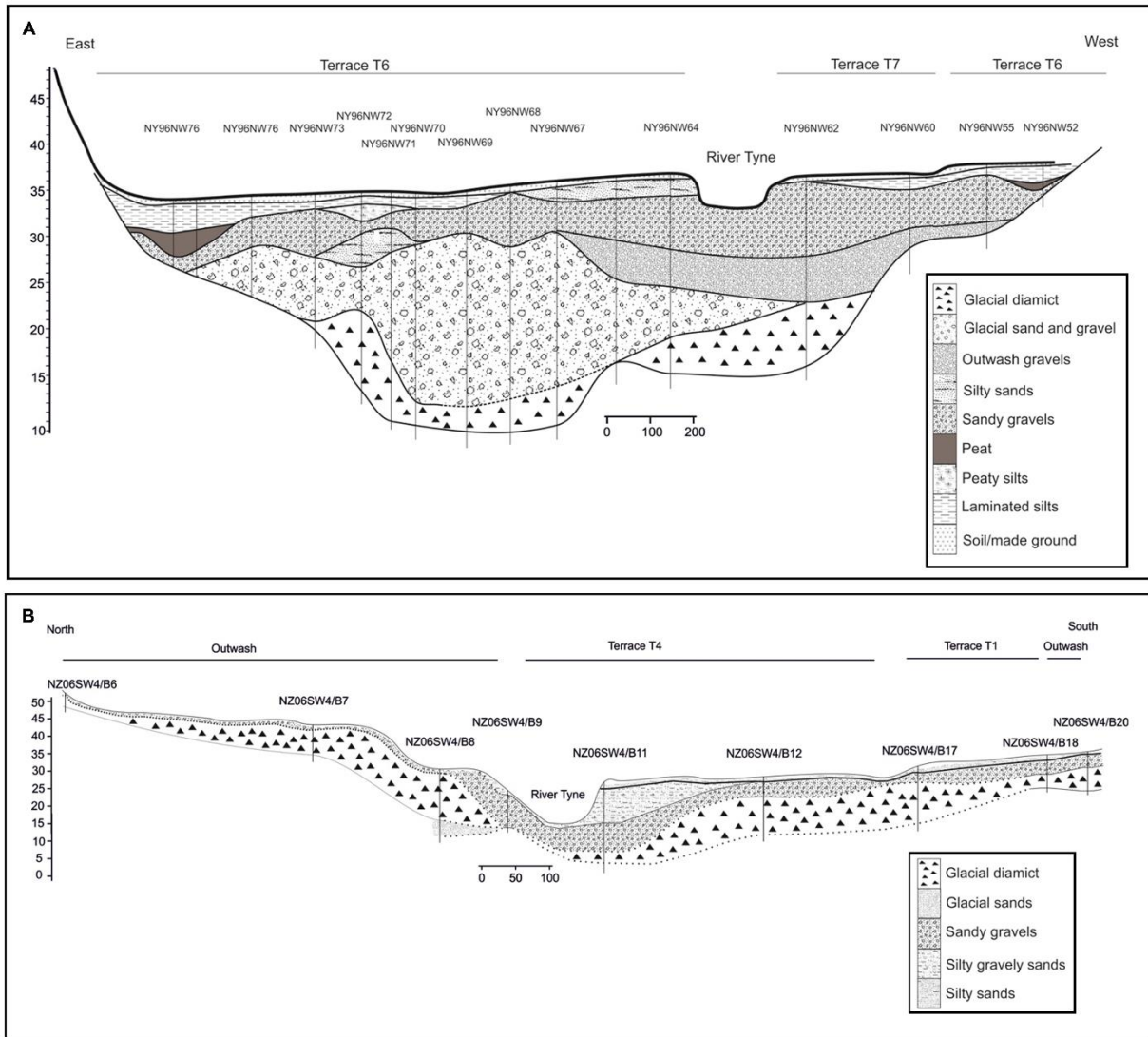
1066

Figure 3. LiDAR (© Environment Agency copyright (2023). All rights reserved) derived height range diagram for the Rivers South Tyne, North Tyne and Tyne in metres above UK Ordnance Datum (OD). Contemporary river long profiles are indicated by the dashed black lines. Differentiated river terraces are labelled T1 to T9 respectively and colour coded as follows: T1 dark blue; T2 light blue; T3 dark green; T4 light green; T5 yellow; T6 orange; T7 dark orange; T8 dashed pink; T9 dotted black lines respectively. Outwash represents the glacigenic terrace sequences (pink line).

1067

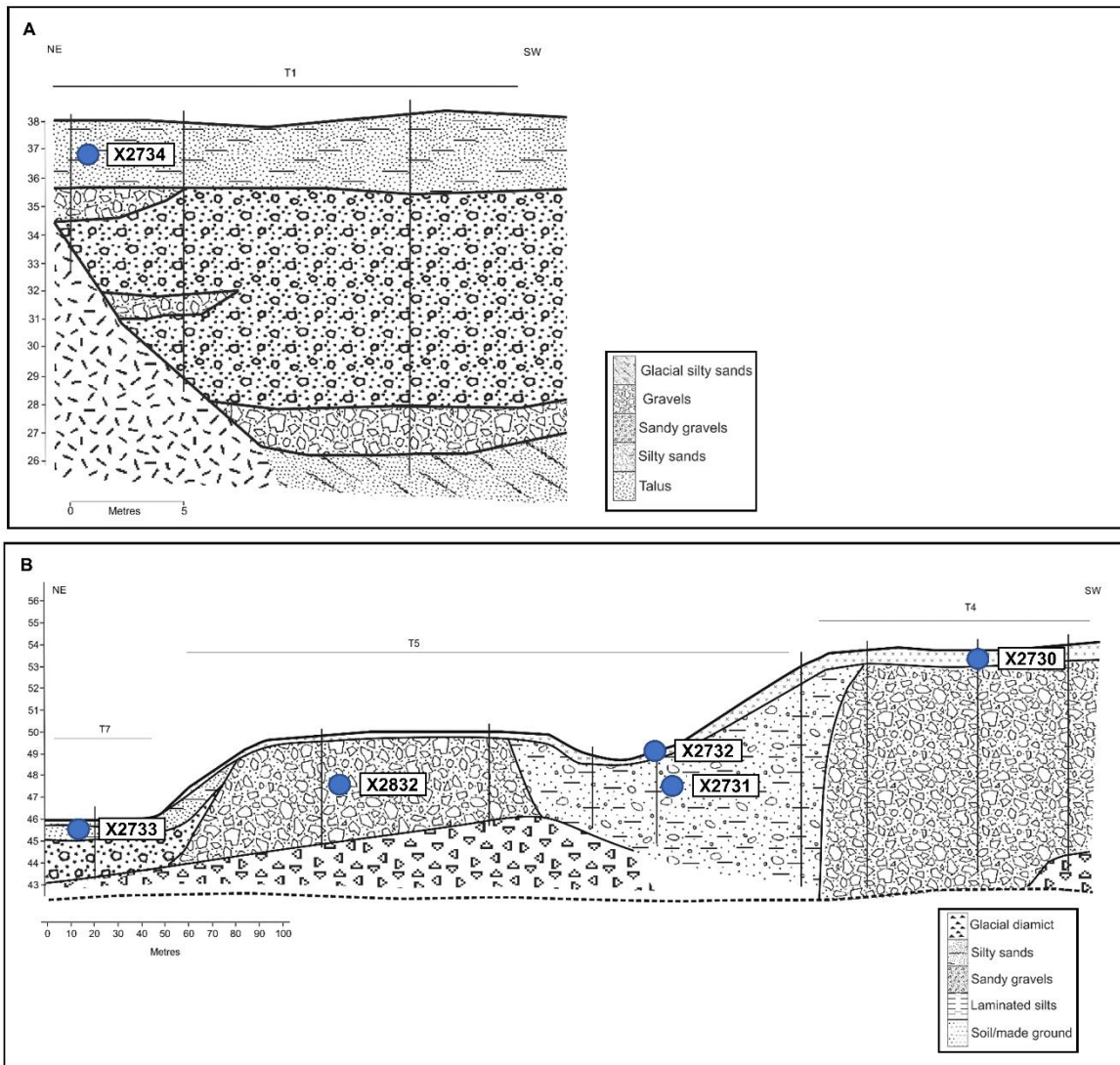
1068

1069 Figure 4. Location of (A) the A69 (road) and (B) the A68 (road) borehole transects, overlain on an  
1070 Ordnance Survey 1: 25 000 Scale Colour Raster (© Crown copyright and database rights 2023  
1071 Ordnance Survey). Showing mapped river terraces, palaeochannels and alluvial fans. AF, alluvial  
1072 fan, T1-8, differentiated river terraces, refer to legend in figure 2.



1073

1074 Figure 5. Detailed stratigraphic and lithofacies assemblages derived from borehole data within  
 1075 zones II and III. (A) the A69 (road) transect, and (B) the A68 (road) transect. Valley-floor transect  
 1076 locations are shown in Fig. 4. Based upon GeoIndex (onshore) Borehole records, with the  
 1077 permission of the British Geological Survey. Individual borehole records demarcated by codes  
 1078 beginning with NY and NZ, with locations indicated by vertical black lines.



1079

1080 Figure 6. Farnley Haugh. (A) T1 alluvium exposed in the cut-bank on the true right-hand side of  
 1081 the valley. (B) Detailed stratigraphic and lithofacies assemblage based upon interpolation of field-  
 1082 gathered vertical profile logs (locations indicated by vertical black lines). The 'X' indicates the  
 1083 sampling location for optically stimulated luminescence dating; lab code X2734. Estimated ages  
 1084 and age ranges are compiled in Table 1.

1085

1086

1087 Figure 7. Fourstones. (A) T5 and T7 alluvium exposed on the true right-hand side of the valley.

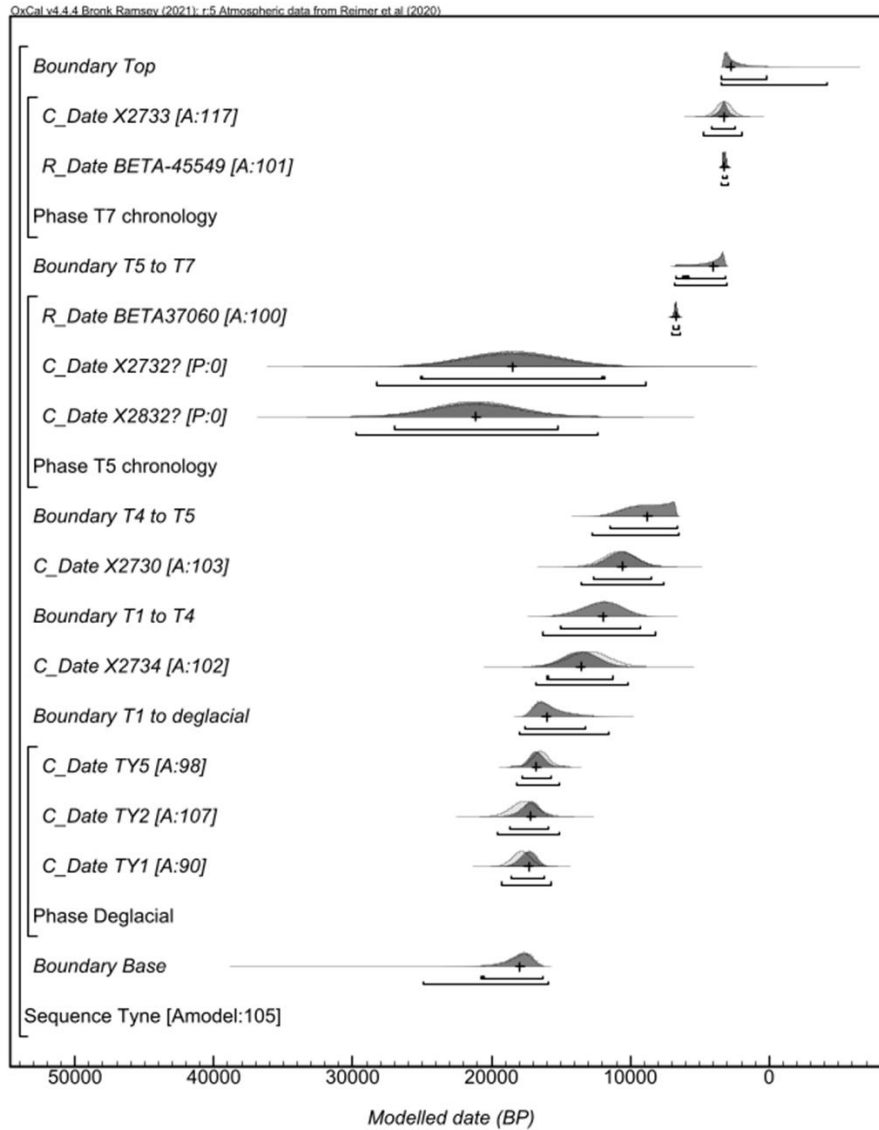
1088 (B) Detailed stratigraphic and lithofacies assemblages based upon interpolation of field-

1089 gathered vertical profile logs (locations indicated by vertical black lines). The 'X' indicates the

1090 sampling locations for Optically Stimulated Luminescence dating; lab. codes X2733 (T7), X2832,

1091 X2732, X2731 (T5), and X2730 (T4). Estimated ages and age ranges are compiled in Table 1.

1092

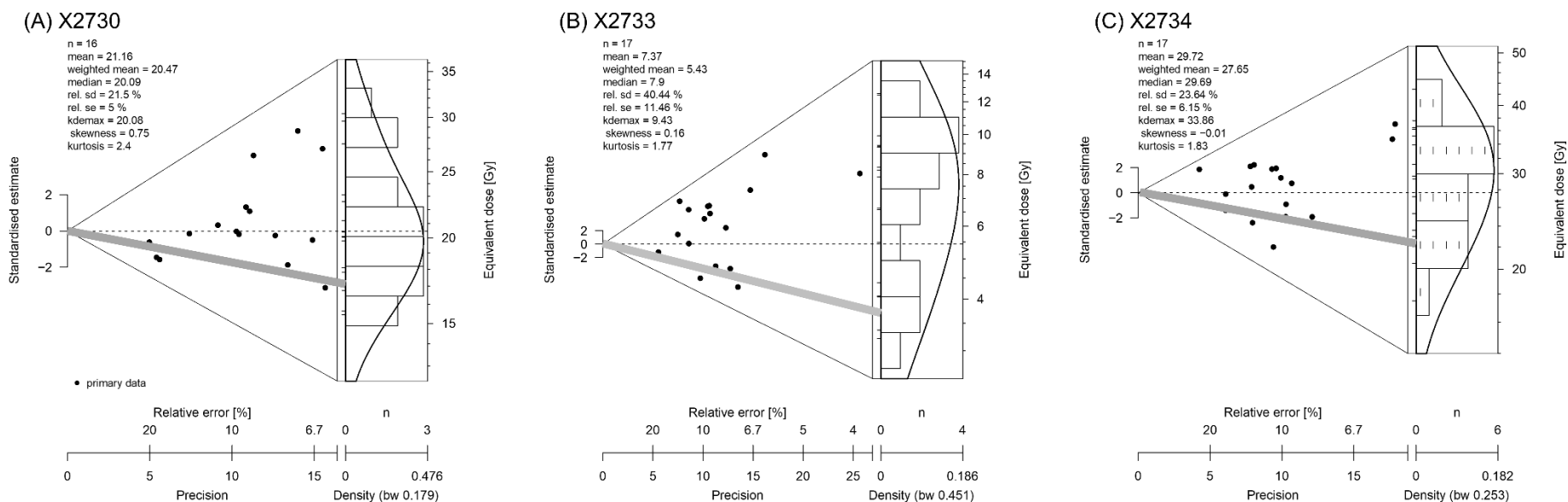


1094

1095 Figure 8. Bayesian model of the dating of the Tyne terrace sequence, based on the new optically  
 1096 stimulated luminescence (OSL) ages obtained by this study, alongside a published <sup>14</sup>C age  
 1097 (BETA-37060; Passmore and Macklin, 1994) and published cosmogenic ages (from boulder for  
 1098 deglaciation of the Tyne Gap Ice Stream (TGIS; Livingstone et al., 2015). The model structure  
 1099 shown used OxCal brackets (left) and key words define the relative order of events (Bronk  
 1100 Ramsey, 2009). Modelled age in ka BP on the x-axis. Each distribution (light grey) represents the  
 1101 relative probability of each age estimate with posterior density estimate (solid) generated by the  
 1102 modelling. Outliers are indicated by '?' and their probability (P) of being an outlier denoted by low  
 1103 values <5 (95% confidence); X2730 not shown as the date is beyond the modelled scale. Model

1104 agreement indices (A) for each age shows their fit to model, with >60% the advocated threshold  
1105 by Bronk Ramsey (2009).





1106

1107

1108 Figure 9. Abanico plots of the individual aliquot equivalent does ( $D_e$ ) values determined for optically stimulated luminescence dating. Plots shown are  
 1109 for samples taken at (A) Fourstones X2730 (T4) and (B) Fourstones X2733 (T7), and at (C) Farnley Haugh X2734 (T1). The plots comprise two parts  
 1110 (i) a bivariate plot, showing standardised estimates of  $D_e$  values in relation to precision (x-axis), and (ii) a univariate plot, showing the age frequency  
 1111 distribution of  $D_e$  values but this does not give any indication of precision. Both plots are linked by the z-axis of the  $D_e$  values. Data points (or primary  
 1112 data) are indicated by the black dots. Age estimates for the samples shown were determined using the MAM  $D_e$ ; the black line across the plots  
 1113 represents the MAM  $D_e$  value for that sample. The abanico plots enable assessment of the data precision and the characteristics of the age  
 1114 distribution; samples with a greater range of  $D_e$  values on the x-axis have a larger scatter in the  $D_e$  distribution. Samples that are well bleached before  
 1115 burial typically have more symmetrical  $D_e$  distributions.

1116 **Table 1.** Summary of new optically stimulated luminescence (OSL) estimated ages and associated information for five samples from  
 1117 Fourstones (south Tyne) and one sample from Farnley Haugh (Tyne). The table includes the total number of aliquots measured with OSL that  
 1118 passed the acceptance criteria and the overdispersion of the resulting dose distribution. Measurements were made on dried, homogenized and  
 1119 powdered material by ICP-MS/AES with an assigned systematic uncertainty of  $\pm 5\%$ . Dry beta dose rates calculated from these activities were  
 1120 adjusted for the field water content and dose rate and age calculations were obtained using DRAC ver1.2 (Durcan et al. 2015).

Location	Lab code	Depth (m)	W* (%)	Cosmic dose rate (Gy/ka)	Total dose rate (Gy/ka)	Aliquots accepted (measured)	Equivalent dose <sup>+</sup> (Gy)	Over-dispersion (%)	Age estimate <sup>++</sup> (ka)
<b>Fourstones</b>	X2730	0.70	18	0.19 $\pm$ 0.02	1.91 $\pm$ 0.02	16 (18)	21.09 $\pm$ 2.04	17.10	10.77 $\pm$ 1.13
	X2731	5.50	18	0.11 $\pm$ 0.01	0.90 $\pm$ 0.06	14 (18)	57.67 $\pm$ 10.89	35.70	61.98 $\pm$ 11.98
	X2732	2.00	18	0.16 $\pm$ 0.01	0.98 $\pm$ 0.06	17 (18)	18.54 $\pm$ 3.29	53.60	18.51 $\pm$ 3.36
	X2733	0.90	18	0.19 $\pm$ 0.02	1.22 $\pm$ 0.08	17 (17)	4.03 $\pm$ 0.66	41.70	3.24 $\pm$ 0.54
	X2832	3.00	24	0.14 $\pm$ 0.01	2.56 $\pm$ 0.17	11 (12)	57.18 $\pm$ 7.78	22.80	21.13 $\pm$ 2.99
<b>Farnley Haugh</b>	X2734	2.00	12	0.16 $\pm$ 0.01	2.45 $\pm$ 0.01	17 (17)	28.80 $\pm$ 2.96	20.40	12.96 $\pm$ 1.44

1121  
1122

1123 \* The recorded moisture contents (values in brackets) are not considered to be representative of the mean water content of the sediment  
 1124 during the burial period as a result of recent (<20years) bank migration and/or quarrying activity. The dose rate calculations are based on  
 1125 more realistic saturation estimates with an associated error of  $\pm 5\%$ .

1126 + OSL measurements were made with an automated TL/DA-15 Risø luminescence reader (Bøtter-Jensen, 1997; Bøtter-Jensen et al., 2000)  
 1127 and conducted on 180–250 $\mu$ m or 90-125 $\mu$ m diameter quartz grains mounted as multigrain aliquots (n=12-17). The equivalent dose (De) was  
 1128 obtained using a single-aliquot regeneration (SAR) measurement protocol (Murray and Wintle, 2000; Wintle and Murray, 2006) and was based  
 1129 on a minimum age model after Galbraith et al. (1999).

1130

1131 ++ The age datum refers to AD 2007 when the samples were measured and the luminescence dates. The total uncertainty ( $1\sigma$ ), calculated  
1132 as the quadratic sum of the random and systematic errors, includes all measurement uncertainties as well as a relative error of 2% to  
1133 account for possible bias in the calibration of the laboratory beta source.